Syndecan-2 is a novel ligand for the protein tyrosine phosphatase receptor CD148

James R. Whiteford[a,b], Xiaojie Xian[b], Claire Chaussade[c], Bart Vanhaesebroeck[c], Sussan Nourshargh[a], and John R. Couchman[b]

[a]Centre for Microvascular Research, William Harvey Research Institute, Barts and the London School of Medicine and Dentistry, Queen Mary University of London, London EC1M 6BQ, United Kingdom; [b]Department of Biomedical Sciences, Copenhagen University, 2200 Copenhagen N, Denmark; [c]Centre for Cell Signalling, Institute of Cancer, Queen Mary University of London, London EC1M 6BQ, United Kingdom

ABSTRACT **Syndecan-2 is a heparan sulfate proteoglycan that has a cell adhesion regulatory domain contained within its extracellular core protein. Cell adhesion to the syndecan-2 extracellular domain (S2ED) is β1 integrin dependent; however, syndecan-2 is not an integrin ligand. Here the protein tyrosine phosphatase receptor CD148 is shown to be a key intermediary in cell adhesion to S2ED, with downstream β1 integrin–mediated adhesion and cytoskeletal organization. We show that S2ED is a novel ligand for CD148 and identify the region proximal to the transmembrane domain of syndecan-2 as the site of interaction with CD148. A mechanism for the transduction of the signal from CD148 to β1 integrins is elucidated requiring Src kinase and potential implication of the C2β isoform of phosphatidylinositol 3 kinase. Our data uncover a novel pathway for β1 integrin–mediated adhesion of importance in cellular processes such as angiogenesis and inflammation.**

Monitoring Editor
Mark H. Ginsberg
University of California, San Diego

Received: Feb 3, 2011
Revised: Jul 21, 2011
Accepted: Jul 25, 2011

INTRODUCTION

Cellular adhesion to the extracellular matrix is an essential feature in developmental processes, tissue repair, inflammation, and immune surveillance. The principal drivers of these processes are integrins; however an important emerging awareness is that cell surface receptor families such as tetraspanins, receptor tyrosine kinases, and growth factor and cytokine receptors can cooperate with integrins to modulate cell behavior and cell fate (Streuli and Akhtar, 2009). The syndecans are another such family of cell surface receptors that function in close association with integrins (Couchman, 2003, 2010). Syndecans are a four -member family of heparan sulfate proteoglycans with roles in cell adhesion, migration, and growth factor and cytokine signaling (for reviews see Alexopoulou *et al.*, 2006; Morgan *et al.*, 2007; Okina *et al.*, 2009; Couchman, 2010). Each syndecan family member has a distinctive expression profile, and despite regions of sequence homology they have distinct sequence motifs suggestive of discrete functionality (Kim *et al.*, 1994). Of relevance to this work is syndecan-2, which is expressed principally in fibroblasts and cells of the vasculature (Marynen *et al.*, 1989; Essner *et al.*, 2006; Fears *et al.*, 2006). Syndecan-2 has roles in left–right axis development in *Xenopus* and also affects branching angiogenesis and matrix deposition and assembly in the developing zebrafish embryo (Chen *et al.*, 2002; Kramer and Yost, 2002; Arrington and Yost, 2009). The effects of syndecan-2 on angiogenesis and matrix deposition have also been established in cell culture systems (Klass *et al.*, 2000; Galante and Schwarzbauer, 2007; Noguer *et al.*, 2009).

Syndecan-2, like other members of the family, has a short, conserved cytoplasmic domain consisting of two highly conserved subdomains (C1 and C2) that flank a more variable V region. The C-termini of the membrane distal C2 domain is a canonical PDZ binding motif, which, in common with other syndecans, interacts with proteins containing PDZ domains such as syntenin, CASK/LIN, and GIPC/synectin (Grootjans *et al.*, 1997; Hsueh *et al.*, 1998; Gao *et al.*, 2000). The membrane proximal C1 domain of syndecan-2 interacts with the actin-binding protein ezrin and is believed to provide a link between syndecan-2 and the actin cytoskeleton (Granés *et al.*, 2000). Syndecan-2 induces dendritic spine formation in hippocampal neurons, and this depends on phosphorylation of the syndecan-2 cytoplasmic domain by the tyrosine kinase receptor

This article was published online ahead of print in MBoC in Press (http://www.molbiolcell.org/cgi/doi/10.1091/mbc.E11-02-0099) on August 3, 2011.

The authors declare that they have no conflicting interests.

Address correspondence to: James R. Whiteford (j.whiteford@qmul.ac.uk).

Abbreviations used: HS, heparan sulfate; NGS, normal goat serum; PI3K, phosphatidylinositol 3 kinase.

EphB (Ethell and Yamaguchi, 1999; Ethell et al., 2001). In colon carcinoma cells syndecan-2 expression affects adhesion, proliferation, and tumorigenic activity (Contreras *et al.*, 2001; Park *et al.*, 2002; Fears *et al.*, 2006).

Many syndecan functions are mediated by interactions with their heparan sulfate (HS) chains—for example, the interaction between syndecan-4 HS and the heparin-binding domain of fibronectin (FN). This interaction, in concert with α5β1 integrin, promotes focal adhesion formation in fibroblasts and depends on syndecan-4 signaling (Saoncella *et al.*, 1999; Woods *et al.*, 2000; Couchman, 2003; Morgan *et al.* 2007). However, syndecans can also promote integrin-mediated cell responses through interactions with regulatory sequences contained within their extracellular core protein. The syndecan-1 ectodomain interacts directly with both αVβ3 and αVβ5 integrin (Beauvais *et al.*, 2004, 2009; McQuade *et al.*, 2006), resulting in cell spreading of MDA-MB-231 cells when syndecan-1 is clustered by cognate antibodies in cell adhesion assays. In addition, blockade of this interaction using a peptide corresponding to residues 82–130 of the syndecan-1 ectodomain results in reduced angiogenesis in murine models (Beauvais *et al.*, 2009). The extracellular domains of both syndecan-2 (S2ED) and syndecan-4 (S4ED) when expressed as glutathione S-transferase (GST) fusion proteins support cell attachment and spreading (McFall and Rapraeger, 1997; McFall and Rapraeger, 1998; Whiteford and Couchman, 2006; Whiteford *et al.*, 2007). Cell adhesion to S4ED requires β1 integrins and a conserved NXIP motif in the syndecan core protein but does not require either endogenous syndecan-4 or heparan sulfate (Whiteford and Couchman, 2006; Whiteford *et al.*, 2007).

The NXIP motif is not present within the sequence of S2ED, and competition assays with S2ED and S4ED proteins demonstrate that the receptor requirements for adhesion to S2ED are distinct from those required for adhesion to S4ED (Whiteford *et al.*, 2007). Fibroblasts form focal adhesions in response to the syndecan-2 ectodomain, but the underlying mechanism remains unclear, other than a requirement for Rho small GTPases and Rho kinase (Whiteford *et al.*, 2007). Integrins are essential for this process since adhesion to the syndecan-2 ectodomain was completely ablated by the presence of β1 integrin–blocking antibodies. In Jurkat cells, phorbol ester–stimulated adhesion to S2ED is blocked not only with the addition of β1-blocking antibodies but also with antibodies specific to the α4 subunit. The syndecan-2 ectodomain is not a α4β1 integrin–specific ligand since many of the cell lines that adhere to S2ED do not possess the α4 subunit, and direct binding assays using recombinant α4β1 in conjunction with S2ED revealed no interaction (Whiteford *et al.*, 2007). This led us to speculate that an alternative cell surface receptor mediates the interaction between β1 integrins and the syndecan-2 ectodomain.

Here we map the adhesion regulatory domain in syndecan-2 and identify the syndecan-2 ectodomain as a ligand for the protein tyrosine phosphatase receptor CD148. We propose that adhesion to this substrate occurs through CD148 signaling to β1 integrin via a process involving both dephosphorylation of the p85 subunit of phosphatidylinositol 3 kinase (PI3K) and the activity of the class II PI3K-C2β in a Src kinase–dependent process.

RESULTS

The adhesion-promoting activity of the syndecan-2 ectodomain resides in the juxtamembrane region

A GST fusion protein encompassing almost the entire ectodomain of syndecan-2 supports cell adhesion, whereas GST alone does not (Whiteford *et al.*, 2007). To map which regions of the syndecan-2 ectodomain regulate cell adhesion, a series of proteins containing in-frame deletions within the murine syndecan-2 ectodomain were used as substrates in adhesion assays (Figure 1, A and B). Deletion of the N-terminal region (from residue E^{19} to L^{73}) of S2ED containing the GAG substitution sites had no effect on fibroblast adhesion, thus confirming that the adhesion regulatory domain of syndecan-2 is located in an equivalent position to that of syndecan-4 (i.e., between the GAG substitution sites and the transmembrane domain) (McFall and Rapreager, 1997, 1998). Further deletions within the 69–amino acid region of syndecan-2 between Q^{72} and F^{141} revealed that cell adhesion regulatory activity resides in the C-terminal 18–amino acid region including P^{124} and F^{141}. Mutant syndecan-2 ectodomain fusion proteins in which this region had been deleted (S2EDΔP^{85}-F^{141}, S2EDΔP^{105}-F^{141}, and S2EDΔP^{124}-F^{141}) all failed to support fibroblast attachment and spreading as reflected by adhesion assays (Figure 1, C and D). Fibroblast attachment and spreading were observed only in proteins that contained the 18–amino acid P^{124}–F^{141} region (S2ED, S2ED ΔE^{19}-Q^{72}, S2EDΔL^{73}-G^{123}). This was reproducible for Swiss 3T3 murine fibroblasts, WI38 human lung fibroblasts, primary murine lung fibroblasts (Figure 1C), and the leukocytic cell line U937 after stimulation with phorbol ester (Supplemental Figure S1A). When Swiss 3T3 fibroblasts seeded on either S2ED or S2EDΔL^{73}-G^{123} were processed for fluorescence microscopy, focal adhesion structures (vinculin-containing plaques) were observed at the termini of microfilament bundles (Figure 1E).

Syndecan ectodomains share little sequence homology between family members or between the same family members from different species. Despite bearing little homology to mammalian syndecan-4 ectodomains, the zebrafish syndecan-4 ectodomain supports mesenchymal cell attachment and spreading (Whiteford and Couchman, 2006; Whiteford *et al.*, 2008). To establish whether the adhesion regulatory properties of syndecan-2 were similarly conserved, a peptide (S2CBD) based on the 18–amino acid region of murine syndecan-2 (P^{124}–F^{141}) containing the adhesion regulatory activity was used as a competitor in adhesion assays together with a scrambled peptide (S2CBDscr) based on the same sequence. An 18–amino acid peptide derived from the equivalent part of the zebrafish syndecan-2 ectodomain (zebS2CBD; S^{130}–F^{157}) was compared with its mammalian counterpart. Swiss 3T3 fibroblasts were incubated in the presence of increasing concentrations of each peptide prior to seeding on wells coated with S2ED. Adhesion was reduced in cells coincubated with the murine S2CBD peptide (S2CBD) or the corresponding zebrafish peptide (zebS2CBD; S^{130}–F^{147}). The scrambled peptide had a negligible effect on cell adhesion even at the highest concentrations (Figure 1F). Both mouse and zebrafish S2CBD peptides reduced cell adhesion and spreading, and comparison of the two peptide sequences revealed that there are considerable similarities in the five C-terminal residues of each peptide (Figure 1G). This suggests that the adhesion regulatory properties of S2ED are principally driven by these conserved residues, S(E/D)NLF. To test this, we also generated a peptide based on S2CBD in which the C-terminal four residues DNLF were substituted with AAAA and found that it had no inhibitory effect on fibroblast adhesion to S2ED (Figure 1F), indicating that these residues are important for the adhesion regulatory properties of the syndecan-2 core protein.

S2ED is a ligand for the protein tyrosine phosphatase receptor CD148

Cell adhesion to the ectodomain of syndecan-2 requires β1 integrin. However, syndecan-2 is not an integrin ligand, and we could demonstrate no direct interaction between β1 integrins and either S2ED or S4ED (Whiteford *et al.*, 2007). Therefore we hypothesized that adhesion to the ectodomain of syndecan-2 requires the action of

another cell surface receptor. Protein phosphorylation is an essential mechanism for regulating cellular processes such as cell adhesion and involves numerous protein kinases and counteracting protein phosphatases. Fibroblasts seeded on S2ED formed focal adhesions that stained positive for phosphotyrosine, and we observed increases in the phosphorylation of key focal adhesion components such as paxillin and focal adhesion kinase (Whiteford *et al.*, 2007). In screens of potential signaling pathways the effect of three common protein tyrosine phosphatase inhibitors on adhesion to S2ED was assayed. Pervanadate, phenylarsine oxide, and dephostatin bind irreversibly to the catalytic cysteine required for dephosphorylation of phosphotyrosine residues (Imoto *et al.*, 1993; Vepa *et al.*, 1997). Application of these inhibitors to rat embryonic fibroblasts seeded on S2ED resulted in sharply reduced cell attachment and spreading (Figure 2A). Adhesion to both S2ED and FN was reduced in the presence of these inhibitors. Pervanadate and phenylarsine oxide inhibited adhesion to S2ED more efficiently than either sodium vanadate or dephostatin. Dephostatin had a greater effect on fibroblast adhesion to FN substrates than to S2ED. The importance of phosphatase activity to the processes governing adhesion to S2ED led us to investigate whether a protein tyrosine phosphatase receptor might be the intermediary molecule that interacts with S2ED leading to β1 integrin–dependent cell adhesion and spreading. In a small interfering RNA (siRNA) screen of the 207 phosphatase genes in the human genome using Jurkat T cell adhesion to S4ED the protein tyrosine phosphatase receptor CD148 (PTPRJ/DEP1) was identified as being potentially important. This was confirmed for fibroblast interactions with S2ED, as WI38 human lung fibroblasts transfected with a gene-specific siRNA pair targeted to CD148 had significantly reduced adhesion to S2ED (Figure 2, B and C). Transfection of fibroblasts with CD148 siRNAs was confirmed to reduce cell surface expression of CD148 by ~50% (Figure 2D). Down-regulation of CD148 in lung fibroblasts had no effect on cell adhesion in response to FN, and transfection of control siRNAs had no effect on adhesion to either S2ED or FN (Figure 2C). U937 cells, which also adhere to S2ED after phorbol ester stimulation, were shown by fluorescence-activated cell sorting (FACS) analysis to express CD148 (Supplemental Figure S1B).

CD148 is a single-pass, membrane-spanning receptor consisting of a single cytoplasmic phosphatase domain and an extracellular domain consisting of eight type III FN repeats (Figure 3A). The extracellular core protein of the human form contains 33 putative sites of N-glycosylation, and a splice variant whose mRNA encodes the first five N-terminal FN type III repeats is present in the sequence databases. The first five FN type III repeats of CD148 were expressed and purified as recombinant protein (Figure 3B). This recombinant protein (CD148sf) was used in several assays. Fibroblast adhesion to S2ED was compromised in a dose-dependent manner by the presence of soluble CD148sf, with concentrations as low as 10 μg/ml being effective (Figure 3C). Adhesion to FN was not affected by CD148sf at any concentration used, and cell adhesion to S4ED substrates was also largely unaffected, except for a small reduction at the highest CD148sf concentration (Figure 3C). Primary rat lung fibroblast adhesion to S2ED was also inhibited in the presence of CD148sf and the adhesion regulatory peptide S2CBD, indicating that this interaction is also relevant to primary cells (Figure 3D). Solid-phase binding assays on plates coated with S2ED, S4ED, the various S2ED deletion mutants, or GST alone revealed a direct interaction between CD148sf and S2ED but not S4ED or GST. Consistent with the cell adhesion data shown in Figure 1, the S2ED deletion mutants lacking the 18–amino acid adhesion regulatory domain between P^{124} and F^{141} also showed no binding to CD148sf, whereas mutants containing this domain (e.g., S2ED ΔE^{19}-Q^{72} and S2EDΔL^{73}-G^{123}) interacted strongly. These data suggest that CD148 is a key regulator of fibroblast adhesion to S2ED, involving an interaction between the extracellular N-terminal part of CD148 and the 18–amino acid adhesion regulatory motif of S2ED.

CD148 signaling stimulates β1 integrin–dependent cell adhesion and spreading

To further dissect the how CD148 promotes fibroblast adhesion, human lung fibroblasts were seeded on wells coated with murine monoclonal CD148-specific antibodies. WI38 fibroblasts attached and spread in response to this substrate but failed to attach and spread in response to either GST or an isotype control for the CD148 antibody (Figure 4, A and C). The antibody was confirmed to recognize the N-terminal FNIII repeats 1–5 of CD148 by Western blot of bacterial lysates expressing the recombinant domain (Figure 4B). A polypeptide of approximately 50 kDa corresponding to FN III repeats 1–5 was only evident in bacterial lysates in which expression of this protein has been induced. Adhesion to the anti-CD148 antibodies leads to similar cytoskeletal rearrangements in both WI38 and SW3T3 fibroblasts as that observed in cells adhering to S2ED (Figure 4C). Fibroblast adhesion to CD148 antibodies could be abolished by the addition of the CD148sf recombinant protein (Figure 4D). Moreover, adhesion to the CD148 antibody was dependent on β1 integrin since blockade by the AIIb2 antibody resulted in the failure of fibroblasts to attach and spread in response to CD148 clustering. In contrast, αVβ3 integrin function–blocking antibodies had no discernible effect on cell adhesion to CD148 monoclonal antibody. These data replicate cell adhesion to S2ED, which was also sensitive to inhibition of β1 but not β3 integrin (Whiteford *et al.*, 2007).

Treatment of cells with phosphatase inhibitors phenylarsine oxide and pervanadate also compromised cell adhesion and cell spreading on CD148 antibody substrates, just as they had on S2ED substrates (Figure 4D). This indicated the importance of CD148 signaling in promoting adhesion responses. To determine whether these β1 integrin–driven processes occur as a result of interactions between the extracellular domains of CD148 and β1 integrin on the cell surface, we used the recombinant CD148 FN III repeat 1–5 protein as a substrate in adhesion assays, and no cell lines tested attached or spread in response to this protein (Figure 4E). Furthermore, solid-phase binding assays in which binding of α5β1 integrin to FN, S2ED, and CD148sf was measured revealed that only wells coated with FN supported β1 integrin binding. No interaction could be observed between α5β1 and either S2ED or CD148 (Figure 4F). Taken together, these data suggest that the β1 integrin–mediated cellular response to CD148 clustering is due to CD148 signaling and not interactions between these molecules on the cell surface. These data are also consistent with the fact that CD148sf could not compromise cell adhesion to FN substrates (Figure 3C).

Epithelial cell adhesion to S2ED is blocked by sialylation

Adhesion to S2ED is a characteristic of cells of a mesenchymal origin; epithelial cell lines tested fail to interact with this substrate (Whiteford *et al.*, 2007). To determine whether posttranslation modifications such as N-glycosylation were important for adhesion to S2ED, we treated cells with tunicamycin and swainsonine. Tunicamycin inhibits the first step in the process of N-glycosylation and effectively blocks fibroblast adhesion to S2ED (Figure 5A). Similarly, swainsonine, which affects glycoprotein modifications in the Golgi, also had an inhibitory affect on fibroblast adhesion to S2ED (Figure 5B); neither treatment suppressed adhesion to FN at the

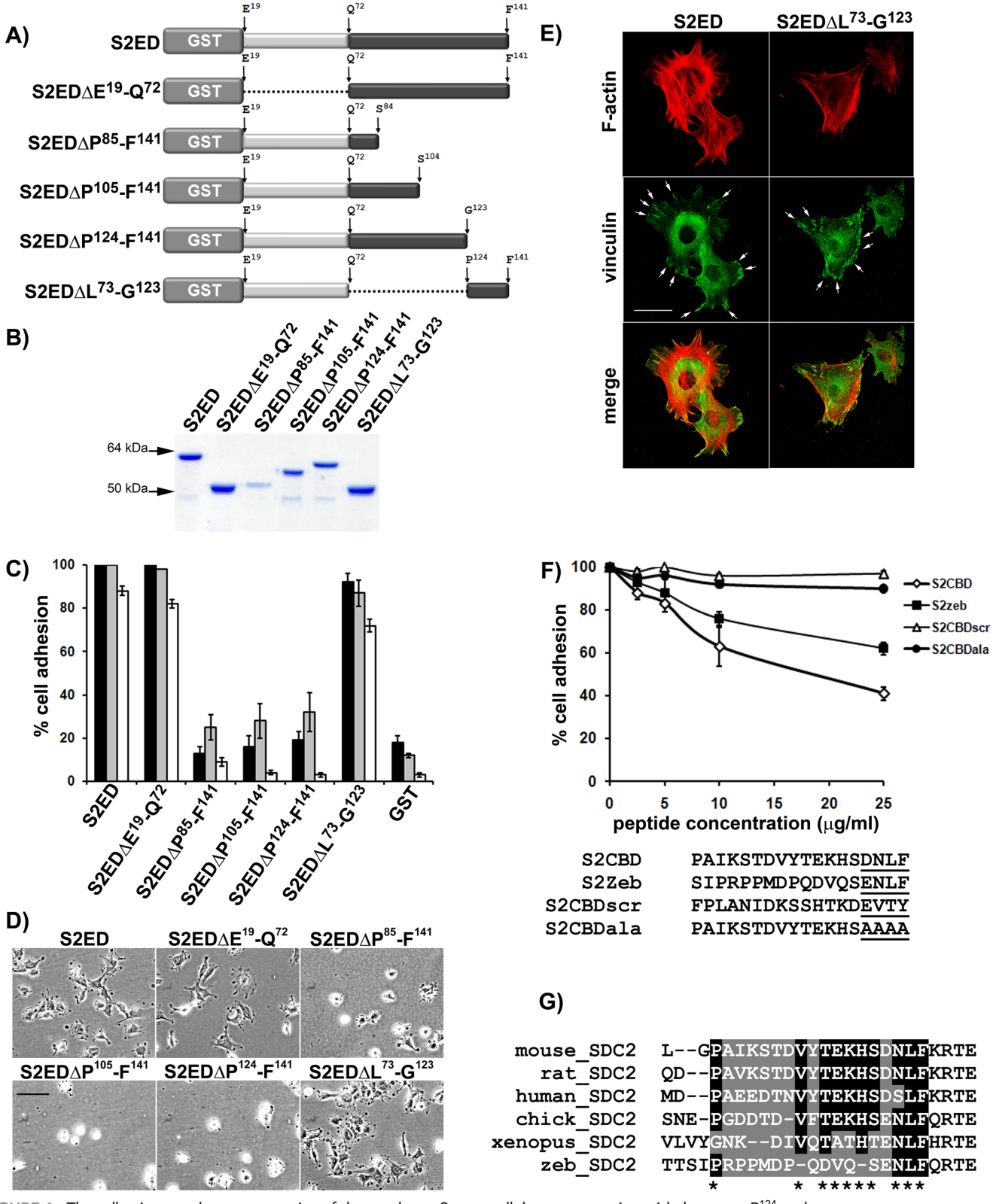

FIGURE 1: The adhesion regulatory properties of the syndecan-2 extracellular core protein reside between P^{124} and F^{141}. Schematic diagram of the mutated forms of S2ED proteins (A) and the purified proteins resolved by SDS–PAGE and stained with Coomassie brilliant blue (B). (C) Wells were coated with each form of S2ED and seeded with either Swiss 3T3 (dark gray bars) or WI38 human lung fibroblasts (light gray bars) or primary murine lung fibroblasts (white bars) in serum-free media. Cell adhesion was measured after 60 min of incubation, and percentage adhesion was calculated relative to adhesion to S2ED, set at 100%. Error bars represent the SD of absorbance measurements made from four separate wells. (D) Phase-contrast micrographs of Swiss 3T3 fibroblasts seeded in serum-free media onto wells coated with each form of S2ED and captured after 60 min (scale bar, 50 μm). Only forms of S2ED that contain the 18–amino acid region of S2ED between Pro^{124} and Phe^{141} support fibroblast attachment and spreading (namely S2ED,

concentrations used. Several molecular interactions are blocked by terminal sialylation of cell surface receptors, and an example is the lymphatic endothelial hyaluronan receptor LYVE-1. When expressed in certain cell types LYVE-1 is incapable of ligand binding, and it is only after treatment with the acetyl-neuraminyl hydrolase neuraminidase that ligand binding occurs (Nightingale *et al.*, 2009). To test whether epithelial cell adhesion to S2ED could be stimulated in epithelial cell lines by the removal of *N*-acetyl-neuraminic acid residues, we treated MDCK cells with neuraminidase. Untreated MDCK cells fail to adhere to S2ED; however, significant attachment and cell spreading occurred in cells treated with this enzyme (Figure 5, C and D). This was also true of the mouse ovarian surface epithelial cell line ID8 and HEK293 cells, which, when treated with neuraminidase, also became adherent to S2ED (Figure 5E and Supplemental Figure S2). However, neuraminidase-treated HEK293 adhesion to S2ED could be inhibited by the addition of the adhesion regulatory peptide (S2CBD), the extracellular portion of CD148 (CD148sf), and blockade of β1 integrin, suggesting that a similar adhesion regulatory pathway exists in epithelial cells but is blocked by sialylation of CD148 (Figure 5E).

Adhesion to S2ED requires Src and PI3K

Proposed substrates for CD148 include Src kinase and PI3K (Pera *et al.*, 2005; Tsuboi *et al.*, 2008). Treatment of fibroblasts with the kinase inhibitors PPI, SU6656, and SrcKI resulted in a reduction in adhesion to S2ED, anti-CD148 antibodies, and FN. However, SrcKI more effectively inhibited adhesion to S2ED than to FN (Figure 6A). These three compounds are known inhibitors of Src kinase activity but also have effects on other key signaling molecules. To further investigate the role of Src kinases in CD148-driven adhesion to S2ED, we performed adhesion assays with mouse embryonic fibroblasts that are null for the Src family kinases Src, Yes, and Fyn (SYF). SYF cells failed to adhere to S2ED, wells coated with anti-CD148 antibodies, or GST but attached and spread in response to FN (Figure 6, B and C). Attachment to S2ED and anti-CD148 antibodies was restored in SYF cells in which Src had been reexpressed (SYF + Src; Figure 6, B and C). To determine whether the failure of SYF cells to attach and spread in response to S2ED or anti-CD148 antibodies was due to the absence of CD148, FACS analysis on both SYF and SYF + Src cells was performed. For both cell types, CD148 expression could be demonstrated on the cell surface. Transient transfection of SYF cells with constructs expressing murine Src, Yes, and Fyn showed that only Src kinase could restore the adhesion pathway to S2ED (Supplemental Figure S3). These data suggest a role for Src kinase in CD148-mediated fibroblast attachment and spreading in response to S2ED. Reports suggested that the C-terminal Tyr-527 of Src kinase is a substrate for CD148 (Pera *et al.*, 2005). However, immunoprecipitations from SYF + Src cells showed no change in Tyr527 phosphorylation levels during adhesion to S2ED (Supplemental Figure S4).

The p85 subunit of PI3K is a proposed substrate of CD148 (Tsuboi *et al.*, 2008). To test the involvement of PI3K, adhesion assays on WI38 and SYF + Src were performed in the presence of the PI3K inhibitor wortmannin (Arcaro and Wymann, 1993). Adhesion to S2ED or anti-CD148 antibodies was prevented by wortmannin in the two cell lines (Figure 7A; WI38 fibroblast data, Supplemental Figure S5). These data suggest a role for PI3K in CD148-mediated adhesion to S2ED, most likely downstream of Src kinase. Immunoprecipitation experiments to establish tyrosine phosphorylation levels of the p85 regulatory subunit of PI3K revealed that it is dephosphorylated after 5 min in SYF + Src cells seeded on S2ED. In contrast, in cells seeded on FN, p85 phosphorylation levels remain unchanged (Figure 7B). Phosphorylation of the p85 subunit of PI3K has been associated with enhanced PI3K activity, and dephosphorylation of p85 could therefore have the opposite effect (Cuevas *et al.*, 2001). Class Ia PI3Ks are heterodimers consisting of a p85 subunit and a p110 catalytic subunit. To determine whether changes in the phosphorylation of the p85 subunit affected PI3K activity, we immunoprecipitated p85-associated PI3K complexes from SYF + Src cell lysates at different time points during adhesion to either S2ED or FN and tested for PI3K activity. The level of class Ia PI3K activity was found to be constant on both substrates at all time points tested (Figure 7C). This suggested that during CD148-mediated adhesion to S2ED, tyrosine phosphorylation of the p85 subunit of PI3K was reduced without down-regulation of its associated kinase activity. Mammals have eight isoforms of PI3K, divided into three classes (Vanhaesebroeck *et al.*, 2010). Wortmannin is a broad-spectrum PI3K inhibitor that affects nearly all members of the PI3K family, with the concentrations used in our assays being in excess of the known IC_{50} values for these kinases (Supplemental Table S1; Chaussade *et al.*, 2007). Given that the class II PI3K isoform PI3K-C2α is not inhibited by wortmannin at the concentrations used (0.01–0.5 μm) (Domin *et al.*, 1997), this PI3K can be excluded as being involved in S2ED-mediated adhesion. To determine whether other PI3K family members were involved in adhesion to S2ED, we tested a second PI3K inhibitor, GDC-0941 (Folkes *et al.*, 2008). This inhibitor has IC_{50} values of ~0.003 and ~0.67 μM for the class I PI3Ks and PI3K-C2β, respectively, with substantially higher IC_{50} for class III PI3Ks (Supplemental Table S1; Folkes *et al.*, 2008). SYF + Src cell adhesion to S2ED was compromised significantly by the presence of ≥1 μM GDC-0941, whereas adhesion to FN was unaffected. Of importance, lower concentrations of this inhibitor, in the dose range that is

S2EDΔE^{19}-Q^{72}, and S2EDΔL^{73}-G^{123}). (E) This adhesion regulatory region also stimulates focal adhesion formation in fibroblasts. Swiss 3T3 fibroblasts were seeded onto glass coverslips coated with either S2ED or S2EDΔL^{73}-G^{123} as indicated, fixed, and stained for the focal adhesion component vinculin (green) and F-actin (red) after 60 min of incubation. Both substrates stimulate focal adhesion formation (denoted by arrows; scale bar, 50 μm). Fibroblast adhesion to S2ED is reduced in the presence of peptides corresponding to murine S2ED (P^{124}–F^{141}) and zebrafish S2ED (S^{130}–F^{147}). (F) Swiss 3T3 fibroblasts were seeded on wells coated with S2ED in the presence of peptides (sequences below graph) corresponding to murine syndecan-2 P^{124}–F^{141} (S2CBD), a scrambled peptide based on this sequence (S2CBDscr), a peptide based on the murine syndecan-2 P^{124}–F^{141} peptide in which the terminal four residues (D^{138}–F^{141}) are substituted with four alanine residues (S2CBDala), and a peptide corresponding to the equivalent region of zebrafish syndecan-2 at the concentrations indicated. Cell adhesion was measured after 60 min of incubation, and adhesion to S2ED in the absence of peptide was set at 100%. Error bars represent the SD of absorbance measurements made from six replicates. Both murine and zebrafish peptides inhibit cell adhesion to S2ED, whereas the scrambled control and the peptide in which the last four C-terminal residues have been substituted with alanine residues have no effect on cell adhesion. (G) Sequence alignments of the syndecan-2 adhesion regulatory domains (highlighted) from several vertebrates reveal few conserved amino acid residues between murine and zebrafish sequences, except for the adhesion regulatory C-terminal SD/ENLF motif.

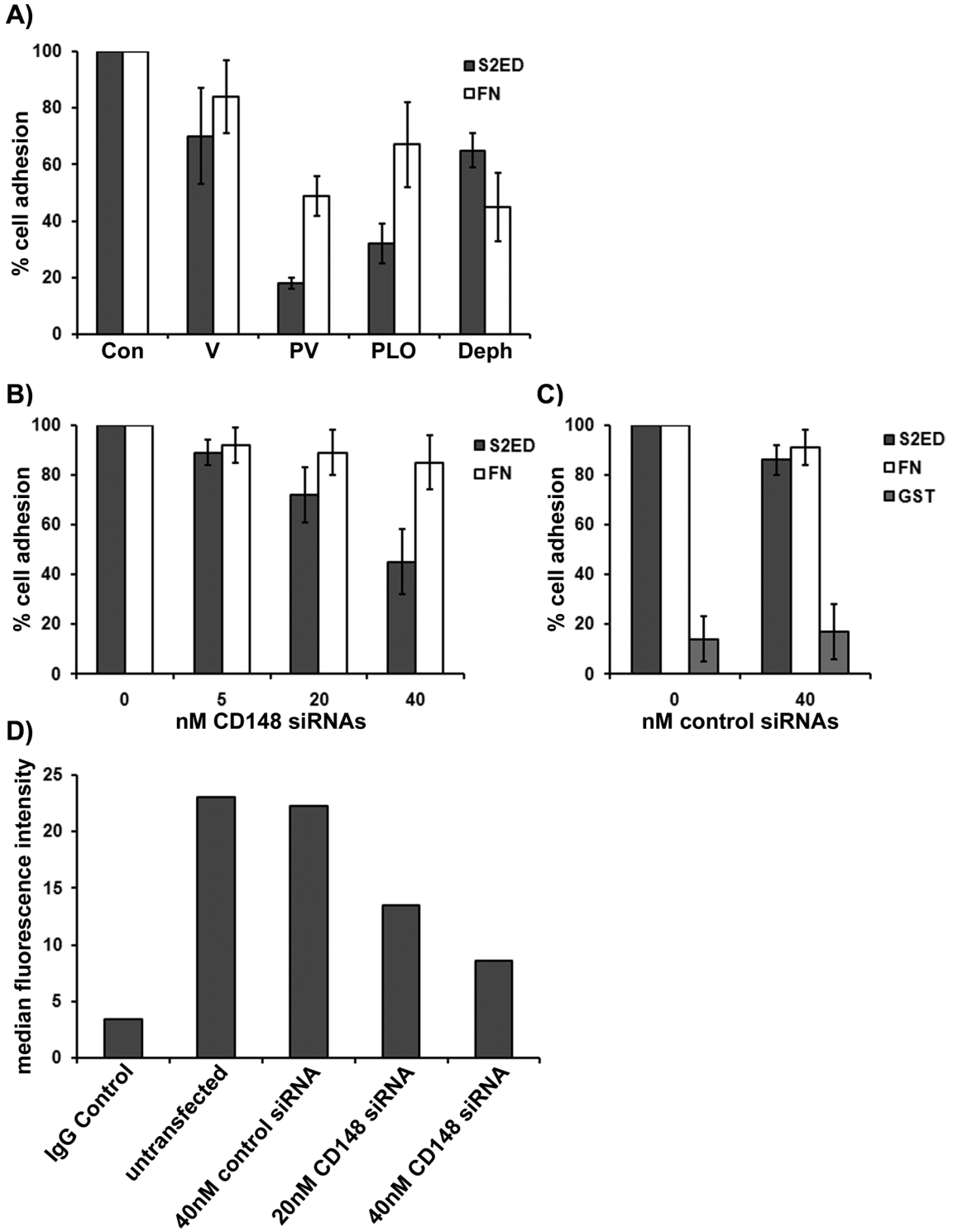

FIGURE 2: Adhesion to S2ED requires the protein tyrosine phosphatase receptor CD148. (A) Protein tyrosine phosphatase inhibitors compromise cell adhesion to the syndecan-2 ectodomain. Rat embryo fibroblasts were seeded in serum-free conditions onto wells coated with either S2ED (dark gray bars) or FN (white bars) as indicated for 60 min in the presence of vanadate (V), pervanadate (PV), phenylarsine oxide (PLO), or dephostatin (Deph). Adhesion is shown relative to cell adhesion to FN and S2ED in the absence of inhibitors, and error bars represent the SD of mean values of four replicates. (B, C) WI38 lung fibroblasts were transfected with a pair of gene-specific CD148 siRNAs at the concentrations indicated (B) or control siRNAs (C) and seeded in serum-free media on wells coated with S2ED (dark gray bars) or FN (white bars). In C, cells were also seeded on wells coated with GST alone (light gray bars). Cells transfected with CD148 siRNAs show reduced adhesion to S2ED compared with control siRNA-transfected cells. Adhesion to FN is unaffected by CD148 siRNAs. Adhesion of control siRNA cells seeded on FN substrates was set at 100%. Error bars represent the SD of absorbance measurements made from triplicates. (D) Knockdown of CD148 in transfected fibroblasts was verified by FACS, which showed a reduction in cell surface CD148 expression. Bar chart indicates the median fluorescence intensity of populations of cells immunostained with CD148 specific antibodies.

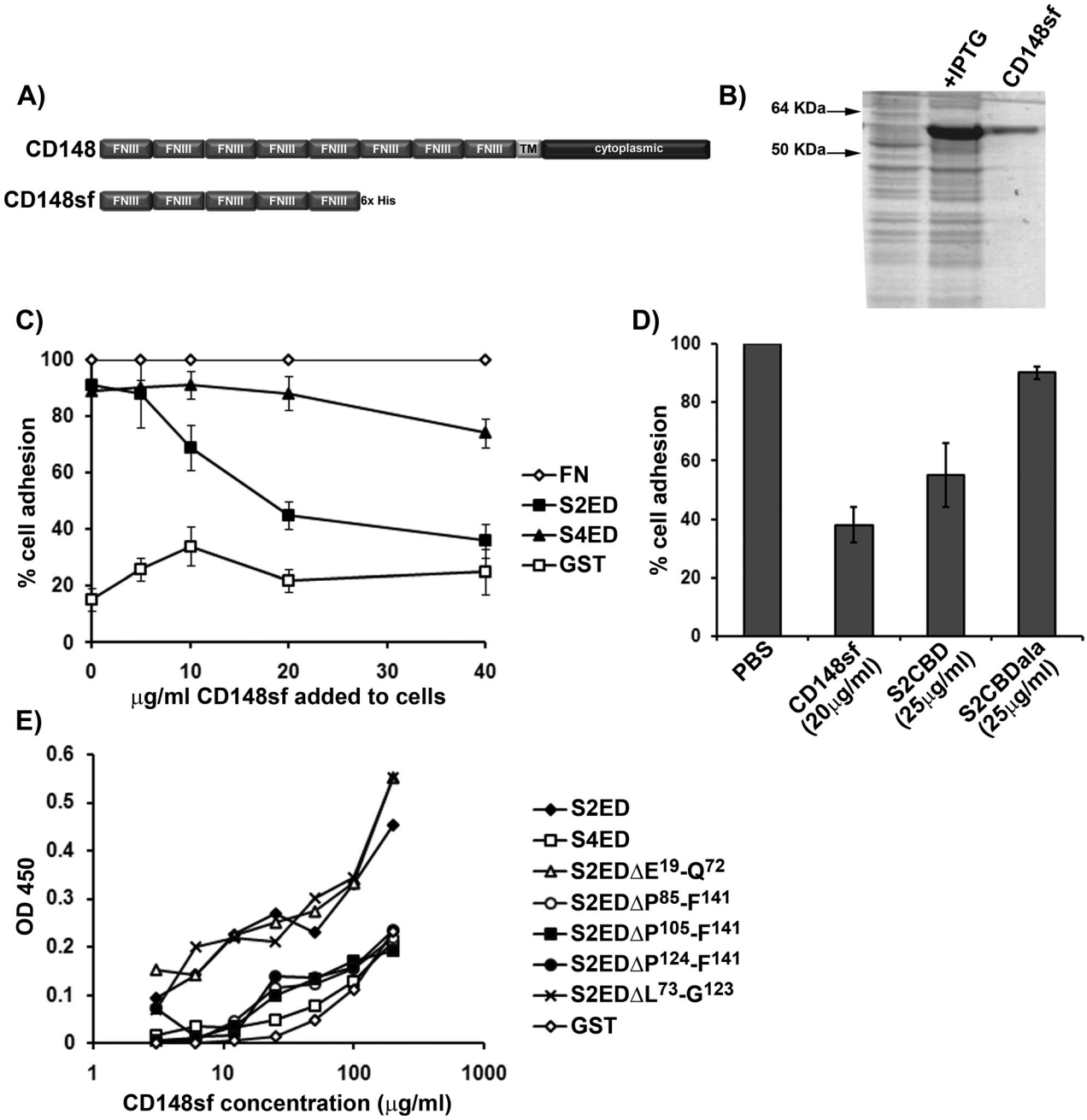

FIGURE 3: The extracellular domain of CD148 interacts with S2ED. (A) Schematic diagram of CD148 showing the extracellular domain comprising eight FNIII repeats, a single transmembrane domain, and a cytoplasmic domain. The first five N-terminal FNIII repeats were cloned and expressed in *E. coli*, and the resultant protein is referred to as CD148sf. (B) Purified CD148sf is shown by SDS–PAGE and Coomassie brilliant blue staining. (C) Incubation of Swiss 3T3 fibroblasts in the presence of CD148sf results in compromised cell adhesion to S2ED. Cells were seeded in serum-free media on wells coated with FN, S2ED, S4ED, or GST in the presence of the indicated concentrations of CD148sf. Adhesion is calculated relative to adhesion to FN in the absence of CD148sf. (D) Adhesion to S2ED by primary rat lung fibroblasts also depends on CD148. Cells were seeded on wells coated with S2ED in serum-free media in the presence of CD148sf, the adhesion regulatory peptide S2CBD, and the negative control S2CBDala at the concentrations indicated. Adhesion is calculated relative to adhesion to S2ED in the absence of competitors. (E) Direct interactions between CD148sf and S2ED are mediated through the adhesion regulatory domain of S2ED. Solid-phase binding assays were performed with wells coated with 200 ng of the substrates indicated and incubated in the presence of increasing concentrations of CD148sf as indicated. The amount of bound CD148sf was quantified using antibodies specific for CD148. CD148sf interacts only with S2ED, S2EDΔE^{19}-Q^{72}, and S2EDΔL^{73}-G^{123}, all of which contain the syndecan-2 adhesion regulatory motif.

expected to block class I PI3Ks (0.01–0.1 μM; Supplemental Table S1) had little effect on adhesion to S2ED, suggesting that an additional PI3K is required for adhesion to S2ED. Inhibition was observed at higher concentrations of the inhibitor (≥1 μM), indicating a possible requirement for the PI3K-C2β isoform of class II PI3K. Alternatively, it is possible that both class I PI3Ks and PI3K-2β need to be

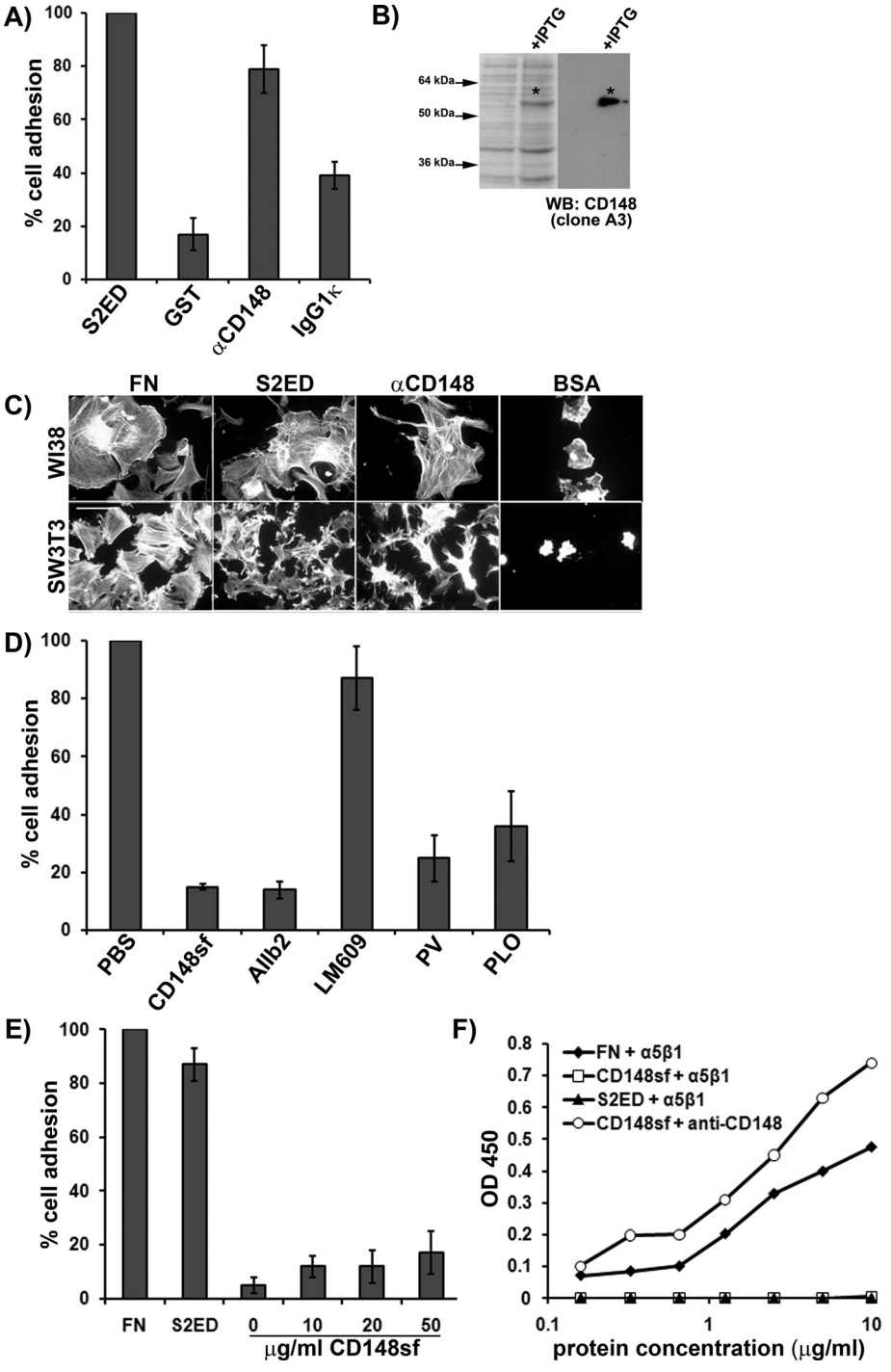

FIGURE 4: Clustering of CD148 with cognate antibodies results in β1 integrin–dependent cell attachment and spreading and requires CD148 signaling. (A) Fibroblasts attached and spread in response to clustering with anti-CD148 antibodies. WI38 lung fibroblasts were seeded in serum-free media on wells coated with S2ED, GST, an anti–human CD148 antibody, or the corresponding murine IgG1κ isotype control. Pronounced adhesion to the S2ED and CD148 antibody is shown. (B) The anti-CD148 antibody specifically recognizes CD148sf, confirming its specificity. Western blot of bacterial lysates from cultures incubated with or without IPTG. The antibody recognizes only CD148sf. (C) Adhesion to anti-CD148 antibodies promotes changes in cytoskeletal organization in WI38 and Swiss 3T3 fibroblasts Cells were seeded on coverslips coated with the substrates indicated in serum-free media and were fixed and stained for F-actin after 60 min (scale bar, 50 μm). (D) Fibroblast adhesion and spreading in response to CD148 antibodies requires β1 integrin and protein tyrosine phosphatase activity. Fibroblasts were seeded on wells coated with anti-CD148 antibodies in serum-free media in the presence of CD148sf (20 μg/ml), β1 integrin function–blocking antibodies (AIIb2), αVβ3 integrin function–blocking antibodies (LM609), or the phosphatase inhibitors pervanadate (PV) and phenylarsine oxide (PLO) as indicated. Blockade of β1 integrin and protein tyrosine phosphatase inhibitors results in compromised fibroblast adhesion. (E) CD148sf does not support human lung fibroblast adhesion, indicating that it is not a ligand for β1 integrin. Fibroblasts were seeded as described on FN, S2ED ,or increasing amounts of CD148sf. Cells failed to attach and spread in response to CD148sf, regardless of concentration. Adhesion of cells seeded on S2ED in A, on anti-CD148 antibodies with no treatment in D, and to FN in E was set to 100% in each case. Error bars represent the SD of absorbance measurements made from five replicates. Recombinant α5β1 integrin does not interact with CD148sf in solid-phase binding assays (F). Assays were performed in 96-well plates coated with FN, CD148sf, or S2ED at the concentrations indicated. The recombinant integrin interacted with FN in a dose-dependent manner. CD148sf coating was verified using anti-CD148 antibodies as indicated.

inhibited to block adhesion to S2ED. Experiments using Src inhibitors, wortmannin, and GDC-0941 also showed that there is a requirement for Src and the PI3K isoforms in primary mouse lung fibroblast adhesion to S2ED (Supplemental Figure S6).

To determine whether the requirement for Src kinase activity occurs upstream or downstream of the requirement for PI3K activity during adhesion to S2ED, we transfected SYF cells with either wild-type or constitutively active avian Src and treated the cells with the PI3K activity inhibitors wortmannin and GDC-0941. SYF cells transfected with vector control, wild-type Src, or Src (Y^{527}-F) all attached and spread to fibronectin, and the administration of wortmannin or GDC-0941 had little effect (Figure 7F). Adhesion to S2ED by SYF cells is restored by the expression of Src and constitutively active Src (Y^{527}-F) but abolished by the addition of wortmannin and GDC-0941 (Figure 7E). This suggests that activated Src is required for adhesion to S2ED upstream of the requirement for PI3K.

DISCUSSION

The adhesion regulatory property of syndecan ectodomains in concert with integrins is mostly associated with syndecan-1 and

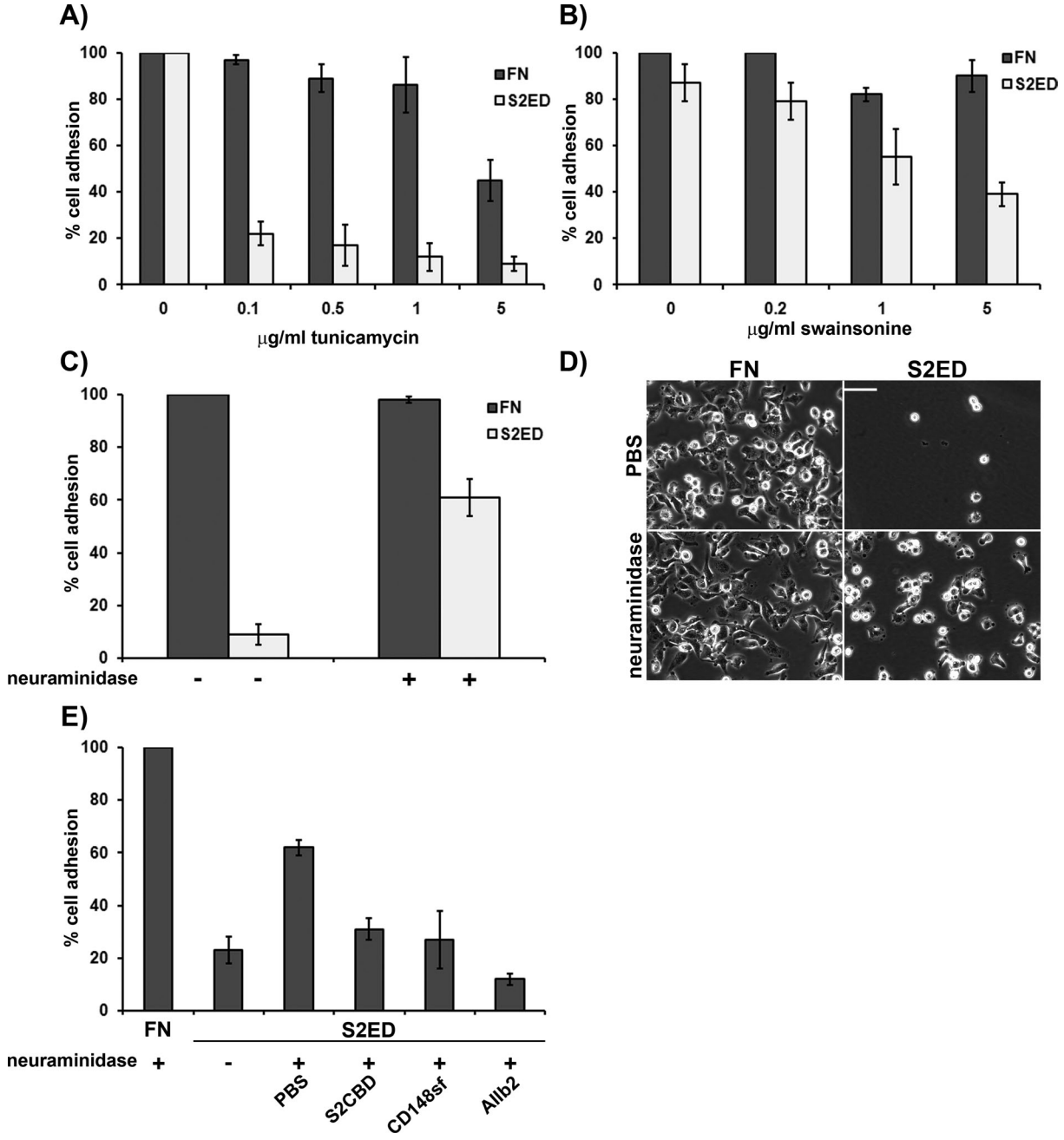

FIGURE 5: Adhesion to S2ED is blocked by sialylation of cell surface receptors. Inhibitors of N-glycosylation, such as tunicamycin (A) and swainsonine (B), block rat embryo fibroblast cell adhesion to S2ED. Fibroblasts were seeded on wells coated with either FN (dark gray bars) or S2ED (light gray bars) for 60 min in the presence of either tunicamycin or swainsonine at the concentrations indicated. Adhesion is shown relative to cell adhesion to FN and S2ED in the absence of inhibitors, and error bars represent the SD of mean values of four replicates. Epithelial cells adhere to S2ED after treatment with neuraminidase (C). MDCK cells were seeded in serum-free media in the presence or absence of neuraminidase (500 U). Cells were incubated for 15 min at 37°C prior to seeding on wells coated with either FN (dark gray bars) or S2ED (light gray bars). Adhesion is shown relative to cell adhesion for untreated cells seeded on FN, and error bars are calculated as described in A and B. Phase-contrast micrographs of MDCK cells seeded on the substrates treated with either PBS or neuraminidase. Removal of sialic acid groups results in cell attachment and spreading. Scale bar, 50 μM. (E) HEK293 cells adhere to S2ED after treatment with neuraminidase, and the process is inhibited by S2CBD, CD148sf, and β1 integrin–blocking antibodies. Cells were seeded on the substrates indicated in serum-free media supplemented with neuraminidase and the S2 adhesion regulatory peptide S2CBD (25 μg/ml), CD148sf (20 μg/ml), or the β1 integrin–blocking antibody AIIb2 (10 μg/ml). Adhesion is calculated as a percentage of total cell adhesion to FN. Error bars represent the SD of five measurements.

syndecan-4 (Beauvais *et al.*, 2004, 2009; Whiteford and Couchman, 2006). However, earlier work showed that S2ED can support mesenchymal cell adhesion in a β1 integrin–dependent process, and when added to microvascular endothelial cells the syndecan-2 core protein promoted cell migration and angiogenic sprouting (Fears *et al.* 2006; Whiteford *et al.*, 2007). Direct interactions between αVβ3

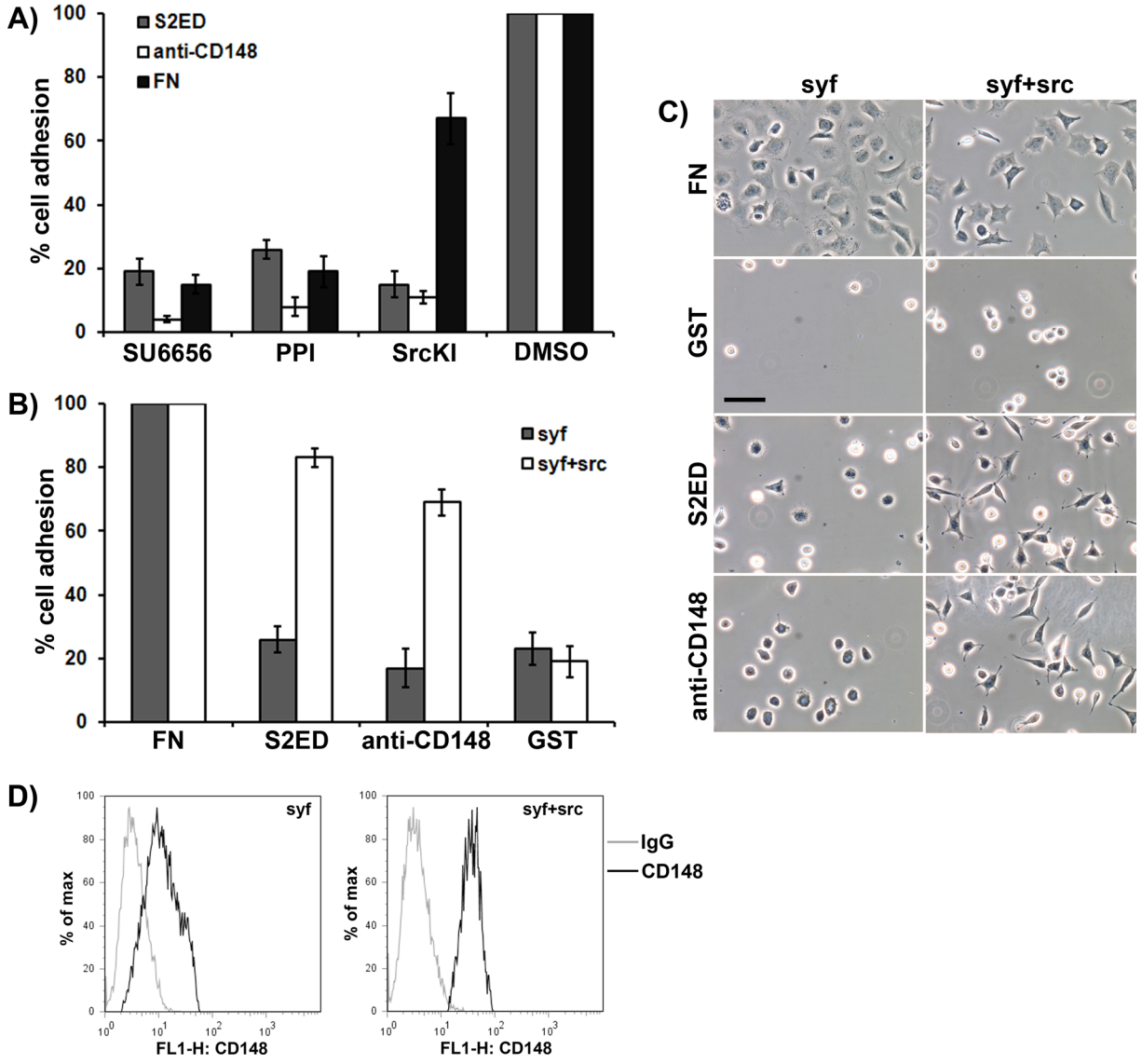

FIGURE 6: Adhesion to S2ED through CD148 requires Src kinase activity. (A) Treatment of rat embryo fibroblasts with the protein kinase inhibitors SU6656, PPI, and SrcKI results in compromised adhesion to S2ED (gray bars), CD148-specific antibodies (white bars), and FN (black bars). Fibroblasts were seeded onto the substrates in serum-free media for 60 min prior to quantification of adhesion. Adhesion in the absence of inhibitors was set at 100%. (B, C) Cells null for the Src family kinases Src, Yes, and Fyn (SYF; gray bars) adhere and spread (C) poorly on S2ED and anti-CD148 antibodies, but these properties are restored by the reexpression of Src in these cells (SYF + Src; white bars). For each cell line adhesion to FN was set at 100%. In A and B error bars represent the SD derived from measurements of five replicates. Phase-contrast micrographs of SYF and SYF + Src cells seeded on the substrates indicated are shown in C (scale bar, 50 μm). (D) Both SYF and SYF + Src cells express CD148 as demonstrated by flow cytometry. Cells stained with CD148 antibodies are denoted by black lines and the IgG controls by gray lines.

or αVβ5 integrin and the syndecan-1 extracellular core protein have been demonstrated (Beauvais *et al*., 2009); however, a similar interaction between syndecan-2 and β1 integrin does not occur (Whiteford *et al*. 2007).

Here we report that adhesion and cytoskeletal organization in response to the extracellular core protein of syndecan-2 require both an interaction with the protein tyrosine phosphatase receptor CD148 and its phosphatase-initiated signaling to promote β1 integrin–mediated fibroblast attachment and spreading (Figure 8). In responsive mesenchymal cells, syndecan-2 core protein is a ligand for CD148, which until now was an orphan receptor. Engagement of CD148 with S2ED and its C-terminal regulatory 18–amino acid region promoted a signaling pathway leading to inside-out integrin activation and focal adhesion formation. In fibroblasts, CD148 was originally identified as density-enhanced phosphatase (DEP1) since it was significantly upregulated in cells at confluency (Ostman *et al*., 1994). In-*trans* interactions between syndecan-2 and CD148 may stimulate cell adhesion and focal adhesion formation as a mechanism to regulate cell proliferation and growth, perhaps consistent with the fact that CD148 has been identified as a tumor suppressor (Keane *et al*., 1996; Ruivenkamp *et al*., 2002; Iuliano *et al*. 2004). However, CD148 null mice grow and reproduce normally, are fertile, and show no enhanced susceptibility to tumor development (Trapasso *et al*., 2006). In epithelial cells, CD148

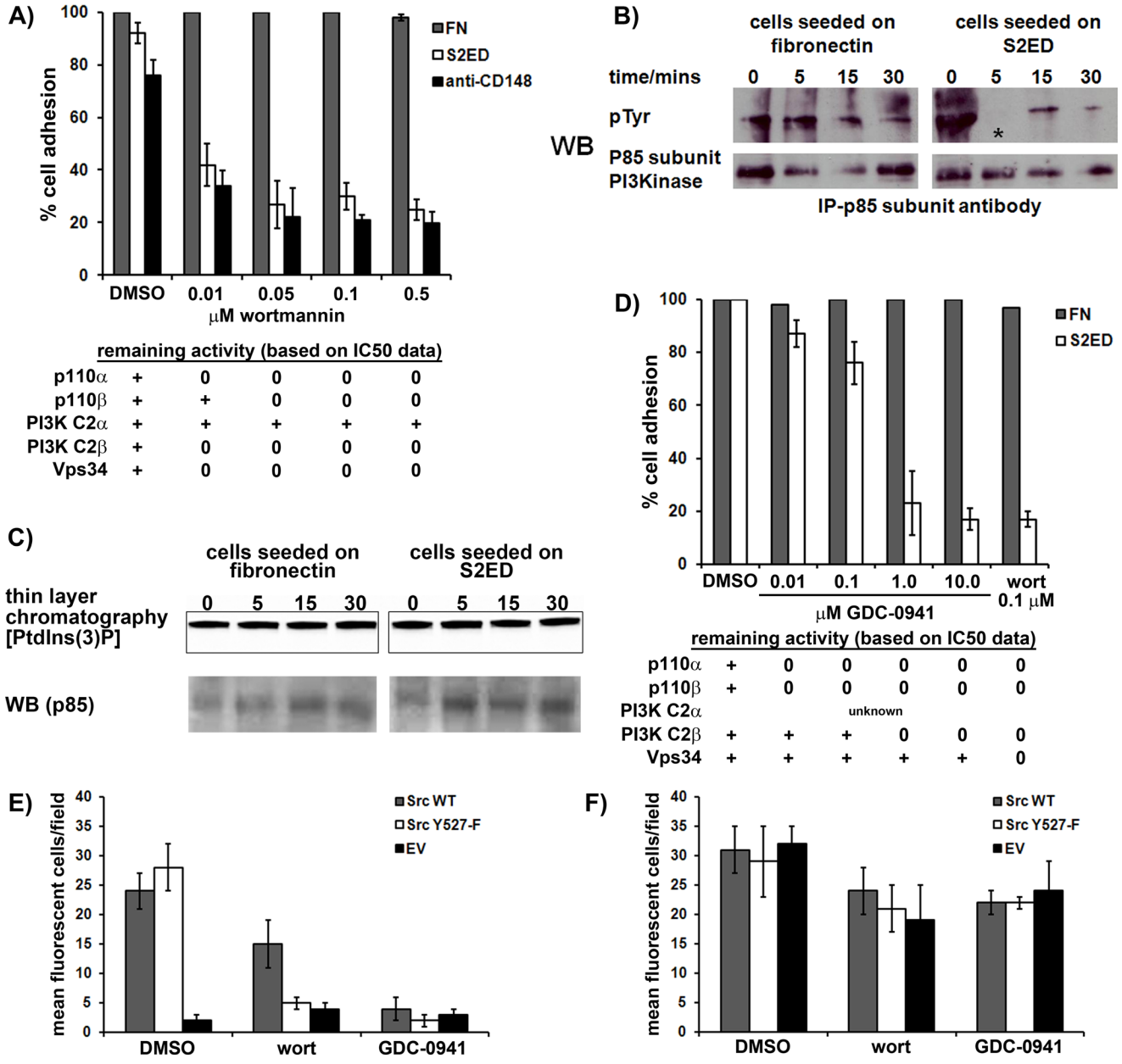

FIGURE 7: Adhesion to S2ED via CD148 requires PI3K activity downstream of Src kinase. (A). SYF + Src cells were seeded in the presence of the indicated concentrations of the PI3K inhibitor wortmannin on FN- (gray bars), S2ED- (white bars), or anti-CD148–coated wells. Adhesion in serum-free conditions for 60 min was quantified. Error bars represent the SD from values obtained from four separate wells per condition. (B). The p85 subunit of PI3K is dephosphorylated early during adhesion to S2ED. The p85 subunit of PI3K was immunoprecipitated from SYF + Src cell lysates harvested at the time points indicated after seeding on either FN or S2ED. Immunoprecipitates were blotted and probed with phosphotyrosine antibodies as indicated. (C) The activity of class Ia PI3K heterodimers remains constant during adhesion to S2ED (top). PI3K complexes were immunoprecipitated using p85-specific antibodies and used in enzyme assays in which phosphatidylinositol 3-phosphate synthesis was measured by incorporation of ^{32}P-P_i. Thin-layer chromatograms of PI3K reactions were visualized by autoradiography. As a loading control, the levels of p85 in each reaction were analyzed by Western blot (bottom). (D) Potential requirement for the class II PI3K-C2β in fibroblast adhesion to S2ED. SYF + Src cells were seeded in the presence of the PI3K inhibitor GDC-0941 at the concentrations indicated. Adhesion to S2ED was compromised at 1 μM GDC-0941, indicative of PI3K-C2β inhibition (Supplemental Table S1). GDC-0941 inhibits class I PI3Ks at much lower concentrations. Adhesion to FN is unaffected at any concentration of GDC-0941. Adhesion to S2ED in the presence of dimethyl sulfoxide (DMSO) is set at 100%. The activities of PI3K isoforms (based on IC_{50} data; Supplemental Table S1) at the concentrations of wortmannin and GDC-0941 used are as indicated in A and D. PI3K-C2β activity is required downstream of Src activation during SYF cell adhesion to S2ED. SYF cells were transfected with either wild-type Src (gray bars), a constitutively active form of Src (Y^{527}-F) (white bars) cloned into a bicistronic expression cassette upstream of eGFP, and an empty vector control (black bars). Transfected cells were seeded for 1 h at 37°C in serum-free media on wells coated with either S2ED (E) or FN (F). Cells were treated with DMSO, 0.01 μM wortmannin, or 1.0 μM GDC-0941 as described. Adherent eGFP-expressing cells were counted in fields at 10× magnification. Data are the mean of five separate fields ± SD.

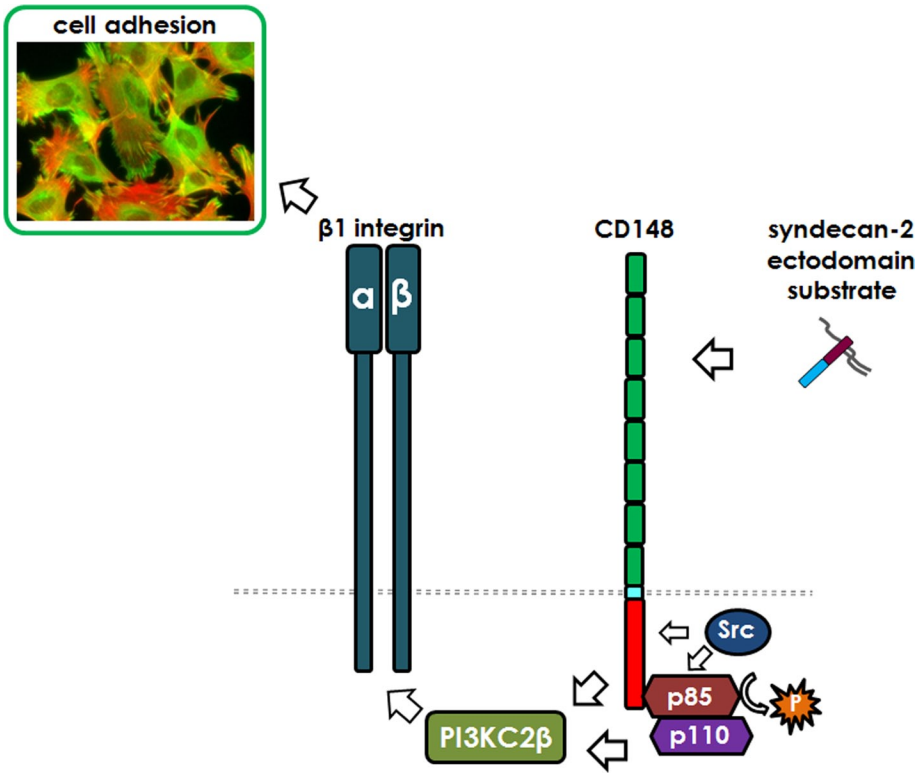

FIGURE 8: The extracellular core protein of syndecan-2 promotes β1 integrin–mediated cell adhesion through interactions with CD148. Schematic model of the interaction between adhesion regulatory elements in the syndecan-2 ectodomain and the protein tyrosine phosphatase receptor CD148 leading to the dephosphorylation of the p85 subunit of PI3K. The interaction requires the action of both Src kinase and PI3K-C2β.

localizes to cell–cell contacts and dephosphorylates the tight-junction proteins occludin and ZO-1 (Sallee and Burridge, 2009). However, tight junctions are not a feature of fibroblasts.

Syndecan-2 null mice have yet to be generated; however, animal models and expression data suggest roles for syndecan-2 in the vasculature, as is also the case for CD148. CD148 null mice have an increased tendency for bleeding and arterial thrombosis, and, as the only PTPR expressed in platelets, CD148 may be a regulator of platelet activation (Senis *et al.*, 2009). Mice expressing a catalytically dead form of CD148 in which the cytoplasmic domain has been substituted die in midgestation due to chronic vascularization failure (Takahashi *et al.*, 2003). Furthermore, roles for zebrafish CD148 in arterial/venous cell fate have been established, and CD148 is important for endothelial cell survival (Rodriguez *et al.*, 2008; Chabot *et al.*, 2009). Syndecan-2 is closely associated with matrix deposition (Klass *et al.*, 2000; Galante and Schwarzbauer, 2007), although both the HS chains and the syndecan-2 cytoplasmic domain are required for this process. Focal adhesions are also sites of matrix deposition and remodeling, and fibroblasts form focal adhesions in response to S2ED. This interaction may also play a role in syndecan-2–mediated matrix deposition, and since syndecans are readily shed by numerous proteinases, matrix-associated syndecan-2 may promote the adhesion pathway described here.

Syndecan-family ectodomain sequences bear little homology to each other, and the putative adhesion regulatory motif of S2ED is not homologous with adhesion-promoting sequences identified in syndecan-1 and -4. The 18–amino acid region lying between P^{124} and F^{141} of murine syndecan-2 does not contain sequence similar to the NXIP motif important for adhesion to S4ED (Whiteford and Couchman, 2006). Neither is it similar to the AVAAV motif or the region corresponding to the bioactive synstatin peptide in the extracellular domain of syndecan-1 (Langford *et al.*, 2005; Beauvais *et al.* 2009). The positions of these regulatory regions in syndecan-1, -2, and -4 in relation to each other are also highly variable. The P^{124}–F^{141} region of syndecan-2 is proximal to the transmembrane domain, whereas in syndecan-4, NXIP resides further toward the N-terminus of the mature protein but C-terminal of the GAG substitution sites. The syndecan-1 ectodomain is much larger than either syndecan-2 or -4 and, in common with syndecan-3, has potential GAG substitution sites situated close to the transmembrane domain. The body of work relating to the adhesion regulatory properties of syndecan-1, -2, and -4 strongly suggests that this is a property of all syndecans. However, the syndecan-3 ectodomain differs in having a mucin homology domain that may be heavily *O*-glycosylated, which might affect such interactions (Carey, 1996). Syndecans are obligate dimers, and this is primarily driven by interactions within syndecan transmembrane domains (Choi *et al.*, 2005). It is possible that the regulatory sequences identified have major structural significance and also regulate dimer formation.

Adhesion to the ectodomain of syndecan-4 is conserved in fish, and we demonstrated here that this applies to syndecan-2. Whether adhesion regulatory domains exist on syndecans from more ancient animals (e.g., *Ciona*) has yet to be established. However, interaction between the *Drosophila* syndecan and the protein tyrosine phosphatase receptor LAR was reported, and this affects synaptic development (Fox and Zinn, 2005; Johnson *et al.*, 2006). However, this interaction requires HS from the *Drosophila* syndecan, and whether direct interactions occur between the two receptors' protein ectodomains is not known. CD148 belongs to a family distinct from LAR, possessing a single phosphatase domain, compared with the tandem catalytic domain of LAR.

The lack of similarity in protein sequence between the syndecan-2 and -4 adhesion-promoting motifs suggests that receptor requirements are specific for adhesion to each protein. Adhesion to S2ED cannot be compromised in competition assays by recombinant S4ED (Whiteford *et al.*, 2007). An initial siRNA array screen of 207 phosphatase genes identified CD148 as being required for phorbol ester–stimulated leukocyte adhesion to S4ED. However, in this study we could show no direct interaction between the N-terminal five FNIII repeats of CD148 and S4ED despite a strong interaction with S2ED. Mature CD148 is heavily N-glycosylated, and we show the importance of these moieties in differentiating between the adhesive characteristics of mesenchymal cells and epithelial cells with regard to cell adhesion to S2ED.

A number of putative PTPRJ substrates have been identified using substrate trapping and overexpression methodologies, including c-Src, PI3K, platelet-derived growth factor receptor, hepatocyte growth factor receptor (cMet), and p120 catenin (Kovalenko *et al.*,

2000; Holsinger *et al.*, 2002; Palka *et al.*, 2002; Pera *et al.*, 2005; Tsuboi *et al.*, 2008). Phosphorylation of CD148 is not well characterized; however, yeast two-hybrid studies demonstrated that the CD148 cytoplasmic domain interacts with the p85 subunit of PI3K but only occurred in yeast expressing a constitutively active Src kinase (Tsuboi *et al.*, 2008). Fibroblast adhesion to both S2ED and cognate CD148 antibodies was compromised in the presence of wortmannin, suggestive of a role for PI3K. Class Ia PI3Ks are heterodimeric proteins comprising an 85-kDa regulatory unit (p85) and a 110-kDa catalytic unit (p110). Under basal conditions the p85–p110 complex is stabilized by interactions involving the SH2 domains of the p85 subunit, leading to inhibition of PI3K activity. Phosphorylation of tyrosine residues within YXXM motifs on receptors and adaptor proteins results binding of the SH2 domains of p85, resulting in alleviation of p85-mediated inhibition of p110, allowing PI3K to phosphorylate its lipid substrates. Interactions between p85 and the CD148 cytoplasmic domain are likely to be via the CD148 catalytic site since substrate-trapping mutants of CD148 capture p85, and although interactions with phosphotyrosines on the cytoplasmic domain may occur, none of the tyrosine residues within the cytoplasmic domain of CD148 lie within a YXXM motif (Tsuboi *et al.*, 2008). The effect of phosphorylation of the p85 subunit on PI3K activity is not clear, although there are reports that p85 tyrosine phosphorylation can lead to an up-regulation of enzyme activity (Cuevas *et al.*, 2001). During the initial phases of adhesion to S2ED as attachment and spreading proceeded, we found rapid dephosphorylation of p85 followed by rephosphorylation. This did not correlate with a reduction in p85-associated PI3K activity during the early phase of adhesion to S2ED (Figure 7C). Our in vitro kinase assays reflect total cellular class Ia PI3K activity, and it is possible that the effects of p85 dephosphorylation on PI3K activity are only localized to adhesion points and any changes in PI3K are masked by the global levels of active kinases within the cell. As adhesion proceeded, p85 phosphorylation was restored. Use of the PI3K inhibitor GDC-0941 in adhesion to S2ED suggested the involvement of a second PI3K family member, PI3K-C2β. This kinase was reported to have roles in cell adhesion, migration, and cytoskeletal rearrangements and also influences the expression of β1 integrin (Domin *et al.*, 2005; Katso *et al.*, 2006).

Our data demonstrated a requirement for activated Src kinase but not the related Yes or Fyn kinases upstream of PI3K in adhesion to S2ED. However, c-Src is apparently not a substrate for CD148/PTPRJ during this process, although CD148 has been reported to dephosphorylate the Tyr-527 residue, leading to up-regulated Src kinase activity (Pera *et al.*, 2005). An alternative hypothesis is that Src kinase is required for phosphorylation of the cytoplasmic domain of CD148, which could be a necessary regulatory step for the phosphatase activity. Its cytoplasmic domain consists of 341 residues comprising a single phosphatase domain and a canonical class II PDZ binding motif at its C-terminus. Contained within this sequence are 20 tyrosine, 19 serine, and 24 threonine residues, many of which are potential sites of phosphorylation. It is also conceivable that Src is required for the phosphorylation of p85 after the initial phases of adhesion to S2ED.

Fibroblast adhesion to the syndecan-2 extracellular core protein can be compromised using β1 integrin–blocking antibodies, but we showed that S2ED is not an integrin ligand. The data demonstrate that cross-talk between cell surface receptors, in this case CD148 and β1 integrin in response to syndecan-2, can lead to cell adhesion responses. Integrins are vital for many aspects of cell behavior, including adhesion, migration, survival, proliferation, and cell fate. The pathway described here provides evidence for a novel role of CD148 in integrin-mediated cell adhesion and suggests that in addition to classic integrin–ligand interactions, other receptors can influence integrin activity status.

MATERIALS AND METHODS

Antibodies and synthetic peptides

The following antibodies were used in this study: β1 integrin function–blocking antibodies AIIb2 (a kind gift from Camilla Fröhlich, University of Copenhagen, Copenhagen, Denmark), αVβ3 function–blocking antibody clone LM609 (Chemicon, Temecula, CA), anti-phosphotyrosine, clone 4G10 (Millipore, Billerica, MA), anti–PI3K p85 (Millipore), anti-vinculin (clone hVIN-1; Sigma-Aldrich, St. Louis, MO), and anti–human CD148 clone A3 (Biolegend, San Diego, CA). The following peptides were obtained from Peptide Protein Research (Wickham, United Kingdom): S2CBD, PAIKSTDVYTEKHSDNLF (corresponding to P^{124}–F^{141} of murine SDC-2); S2CBDscr, FPLANIDKSSHTKDEVTY (scrambled sequence based on S2CBD); zebS2CBD, SIPRPPMDPQDVQSENLF (corresponding to S^{130}–F^{147} of zebrafish SDC-2); and S2CBDala, PAIKSTDVYTEKHSAAAA.

Cells and cell culture

WI38 human lung fibroblasts, rat embryo fibroblasts, fibroblasts lacking the Src, Yes, and Fyn kinases, and those with Src restored were obtained from the American Type Culture Collection (Manassas, VA). All cells were grown and maintained in DMEM (Lonza, Basel, Switzerland) supplemented with 10% fetal bovine serum (Lonza), 2 mM L-glutamine (Invitrogen, Carlsbad, CA), and penicillin (100 U/ml) and streptomycin (100 µg/ml) (Invitrogen). For all experiments cells were maintained at 37°C and 10% CO_2. Primary rat lung fibroblasts were isolated as follows: lungs from 8-wk-old male C57/Bl6 mice were washed three times in sterile phosphate-buffered saline (PBS) before being macerated with a scalpel blade. The resultant lung fragments were placed in a 9-cm dish in DMEM containing 10% fetal bovine serum (FBS) and maintained at 37°C and 10% CO_2. The media was routinely changed every 2 d. After 10 d, fibroblasts were passaged into 25-cm^2 flasks. All cells used in this work were p2 or p3.

Fusion proteins and plasmids

The sequence encoding E^{19}–F^{141} of the murine syndecan-2 extracellular domain was cloned into the bacterial expression vector pET41a (Novagen, Gibbstown, NJ) to form an N-terminal GST–mouse syndecan-2 fusion protein (S2ED) as described in Whiteford *et al.* (2007) (Figure 1A). On the basis of this vector as template, constructs for the expression of syndecan-2 ectodomain mutant GST fusion proteins were generated using a PCR-based approach. Briefly, primer pairs were designed to generate in-frame deletion mutants in which residues E^{19}–Q^{72} (S2EDΔE^{19}-Q^{72}), P^{85}–F^{141} (S2EDΔP^{85}-F^{141}), P^{105}–F^{141} (S2EDΔP^{105}-F^{141}), P^{124}–F^{141} (S2EDΔP^{124}-F^{141}), and L^{73}–P^{124} (S2EDΔL^{73}-P^{124}) were removed from the coding sequence of S2ED (Figure 1A; primer sequences are listed in Supplemental Table S2). Forward and reverse primer pairs corresponding to each mutant were used to PCR amplify S2ED vector DNA, and the resultant PCR products were digested with *Dpn*I for 2 h at 37°C. PCR products were ethanol precipitated, and the pellets were resuspended in water and phosphorylated using T4 polynucleotide kinase. Products were then gel purified, ligated, and transformed into *Escherichia coli* using standard procedures. In-frame deletion of regions within S2ED was verified by DNA sequencing, and plasmids were transformed into *E. coli* strain BL21. Transformed bacterial strains were grown to an OD_{600} of 0.5 prior to the addition of 1 ml/l of 1 M isopropyl-β-D-thiogalactoside (IPTG) and incubated for a further 3 h.

Bacterial pellets were lysed using rLysozyme (Novagen, Gibbstown, NJ) as described by the manufacturer. Fusion proteins were purified using glutathione–Sepharose 4B (GE Healthcare, Piscataway, NJ) as described previously (Whiteford and Couchman, 2006).

The sequence encoding the first five N-terminal FN type III repeats of the extracellular domain of human CD148 was cloned into the *Bam*HI/*Hin*dIII sites of the bacterial expression vector pET24 (Novagen) using standard procedures, and the resultant vector was transformed into *E. coli* strain BL21. The primers used are described in the supplemental figures. Bacteria were grown to an OD_{600} of 0.5 at 37°C prior to the addition of 1 ml/l 100 mM IPTG and incubated for a further 5 h at 30°C. Recombinant CD148 extracellular domain protein was purified using His-Select Nickel Affinity Gel (Sigma-Aldrich) as described by the manufacturer.

Expression constructs encoding full-length avian wild-type c-Src (c-Src-WT) and constitutively active c-Src (c-Src-CA, Y527F point mutation) were previously described (Sanjay *et al.*, 2001; Destaing *et al.*, 2008) and were a generous gift from Marie Kveiborg (University of Copenhagen). cSrc inserts were excised using *Cla*I and *Not*I and the ends filled in using Klenow polymerase prior to ligation into the *Sma*I site of pIRES2–enhanced green fluorescent protein (eGFP; Clontech, Mountain View, CA) using standard procedures. The orientation of inserts was verified by restriction digest, and cells were transfected using lipofectamine as per the manufacturer's protocol. The mammalian expression pCMV-SPORT6 containing full-length cDNAs for murine Src, Yes, and Fyn were obtained from ImaGenes (Nottingham, United Kingdom).

Adhesion assays

Substrates included GST, S2ED, and the mutated forms of S2ED described earlier and anti-CD148 antibody (clone A3; Biolegend). Plates (24 well) were coated overnight with 2.5 μg of each substrate at 4°C. Wells were then washed with PBS prior to the addition of 1% BSA in PBS for 1 h at 37°C. Adherent cells were detached with trypsin (Invitrogen), and cell suspensions were prepared using media containing FBS to inactivate the protease. Cells were pelleted by centrifugation and washed twice in serum-free media, then seeded at 2×10^5 per ml of medium and incubated for 60 min at 37°C. Wells were washed gently with PBS prior to fixation in 0.25 ml of 4% PFA (paraformaldehyde) in PBS for 10 min. Fixed cells were washed three times with PBS and were stained with 0.1% crystal violet in 10% methanol for 20 min at room temperature. Wells were washed three times under running water to remove excess stain before the addition of 0.25 ml/well of PBS and 10 μl of 10% SDS. Plates were shaken gently for 5 min before the OD was measured at 590 nm. In antibody-blocking experiments, cell suspensions in serum-free media were incubated at 4°C for 15 min in the presence or absence of 40 μg/ml antibody prior to seeding onto substrates. Phosphatase inhibitors, Src inhibitors, peptides, and wortmannin (Calbiochem, La Jolla, CA) and GDC-0941 were added prior to cell seeding as described earlier. Sodium pervanadate (1 mM) was prepared as described in Ott and Rapraeger (1998). Phenylarsine oxide and dephostatin were used at 10 and 5 μM, respectively. Src inhibitors were used at the following concentrations; Src kinase inhibitor I, 75 nM (Calbiochem); SU6656, 200 nM (Calbiochem), and PP1, 1 μM (Merck, Darmstadt, Germany). Neuraminidase from *Clostridium perfringens* was obtained from New England Biolabs (Ipswich, MA) and used at a concentration of 50 U/ml.

Flow cytometry

Suspensions of adherent cells were prepared using enzyme-free cell dissociation buffer (Invitrogen) and were washed twice in PBS with 1% normal goat serum (NGS; Invitrogen) and incubated at 4°C for 30 min in the presence of primary antibodies as directed by the manufacturer. Cells were washed twice in PBS with 1% NGS prior to incubation at 4°C for 30 min with the appropriate Alexa Fluor 488–conjugated secondary antibody. After two washes with PBS and 1% NGS, cell populations were analyzed using a BD FACSCalibur flow cytometer (BD Biosciences, Oxford, United Kingdom) and the flow cytometry analysis software FlowJo (Tree Star, Ashland, OR).

Transfection of WI38 cells with gene-specific CD148 siRNAs

WI38 cells were transfected with siRNAs using the HiPerfect reagent (Qiagen, Valencia, CA). The following CD148 gene-specific siRNA sequences were obtained from Qiagen: rj1, [r(UUGAUUGUAGAAGAUACGG)dGdT], SI00044268; and rj2, [r(UAUAGUUAGAUGACGACUC)dGdT], SI00044275. WI38 cells (8×10^4/well) were seeded in a six-well plate for 48 h and then transfected with siRNA pairs (rj1 and rj2) and the AllStars Negative Control siRNA (Qiagen), using each siRNA at the concentration indicated, in conjunction with 5 μl of HiPerfect reagent as described in the manufacturer's instructions. The effects of siRNA treatments on cell surface levels of CD148 were analyzed by FACS 48 h after transfection.

Solid-phase binding assay

Microtiter plate wells were coated overnight with 200 ng of S2ED, S4ED, GST, or the S2ED mutants in PBS prior to blocking in 1% BSA in PBS for 1 h at room temperature. Wells were washed three times with PBS, after which twofold serial dilutions of CD148sf (highest concentration, 200 ng/ml) was added, and left at room temperature for 2 h. Wells were washed three times with PBS, and the plate was incubated with anti-CD148 (clone A3) antibodies (diluted 1:2500 in PBS) for 1 h at room temperature. Wells were washed as described prior to the addition of rabbit anti–mouse immunoglobulin G (IgG) conjugated to horseradish peroxidase (diluted 1:5000 in PBS; Dako, Glostrup, Denmark). After five washes with PBS, TMB One solution (Promega, Madison, WI) was added to each well and the reactions stopped by the addition of 0.1 M hydrochloric acid. The absorbance of each well was measured at 450 nm.

Phase-contrast and immunofluorescence microscopy

Phase-contrast micrographs were captured on an Olympus (Center Valley, PA) IX81 microscope with a Hamamatsu (Hamamatsu, Japan) ORCA-ER digital camera and processed using the Cell software from Olympus and Adobe Photoshop (San Jose, CA). Fibroblasts were immunostained for vinculin and F-actin as described previously (Whiteford *et al.*, 2007). For confocal analysis, the cells were scanned using a Zeiss LSM 5 PASCAL confocal laser-scanning microscope (Zeiss, Welwyn Garden City, United Kingdom) with a 20× (numerical aperture [NA] 0.5 W, PH2) or 40× (NA 0.75 W, PH2) water-dipping Achroplan objective.

Immunoprecipitation and PI3K activity assay

Immunoprecipitation of the p85 subunit of PI3K was performed as follows. Cells were lysed at the time points indicated in buffer (20 mM Tris HCl, pH 7.6, 0.15 M NaCl, 0.1 mM EDTA, 0.1 mM ethylene glycol tetraacetic acid, 1% Triton X-100, and 1× Halt protease and phosphatase inhibitor cocktail [Thermo Scientific, Waltham, MA]) and centrifuged at 15,000 × *g* for 20 min at 4°C. Immunoprecipitation of the p85 subunit of PI3K was performed on lysates using EZ view protein A agarose and specific antibodies as described by the manufacturer (Sigma-Aldrich). For PI3K activity assays, p85 immunoprecipitations were performed as described, and complexes

were used in standard lipid kinase activity assays using phosphatidylinositol as the substrate and ^{32}P-P_i as described by Chaussade *et al*. (2007). TLC plates were quantified using a phosphoimager screen (StormImager, Amersham, Piscataway, NJ).

Phosphatase siRNA array

To determine which phosphatase genes were important for adhesion to S4ED, Jurkat cells were transfected with siRNAs to each of the 207 phosphatase genes in the genome contained within the Human Phosphatase siRNA Array, version 3.0 (Qiagen). The array contains four siRNAs targeted to each phosphatase gene, and in this study pairs of siRNAs for each gene were transfected into cells. Each gene in the array was therefore assayed twice for its effects on Jurkat adhesion to S4ED using independently derived pairs of siRNA sequences. Jurkat cells were diluted to a concentration of 3×10^5 cells/ml of media and grown for 24–48 h before being added to wells of a 24-well plate at a concentration of 2×10^5 cells in 0.1 ml of medium containing serum. siRNA pairs (750 ng of each) were diluted in 0.1 ml of serum-free media, and 6 µl of HiPerfect Transfection Reagent (Qiagen) was added, and the reaction was mixed by vortexing and incubated for 5 min at room temperature. The siRNA transfection mixes were added dropwise to the cells, and the plates were incubated for 6 h prior to the addition of 0.4 ml of normal growth media. For adhesion assays, cells from each well were clarified by centrifugation, washed twice in serum-free media, and resuspended in 0.5 ml of serum-free media containing 10 ng/ml of PMA (phorbol 12-myristate 13-acetate). Cells (0.25 ml) were seeded onto either S4ED- or fibronectin-coated 24-well plates and incubated for 60 min at 37°C before two washes with PBS and fixation with 4% PFA in PBS. Jurkat cells seeded in the presence and absence of PMA were seeded on to every plate coated with both S4ED and FN to serve as positive and negative controls.

ACKNOWLEDGMENTS

This work was funded initially by Wellcome Trust Program Grant 065940 and later by the Danish National Research Foundation, the Danish Medical Research Council, and the Vilhelm Pedersen Fonden through the Novo Nordisk Fonden (to J.R.C.) and by Arthritis Research-UK Grant 19207 to J.R.W. Research in the laboratory of B.V. is funded by Cancer Research UK (C23338/A10200).

REFERENCES

Alexopoulou AN, Multhaupt HA, Couchman JR (2006). Syndecans in wound healing, inflammation and vascular biology. Int J Biochem Cell Biol 39, 505–528.

Arcaro A, Wymann MP (1993). Wortmannin is a potent phosphatidylinositol 3-kinase inhibitor: the role of phosphatidyl 3,4,5-triphosphate in neutrophil responses. Biochem J 296, 297–301.

Arrington CB, Yost HJ (2009). Extra-embryonic syndecan 2 regulates organ primordia migration and fibrillogenesis throughout the zebrafish embryo. Development 136, 3143–3152.

Beauvais DM, Burbach BJ, Rapraeger AC (2004). The syndecan-1 ectodomain regulates alpha (v) beta 3 integrin activity in mammalian carcinoma cells. J Cell Biol 167, 171–181.

Beauvais DM, Ell BJ, McWhorter AR, Rapraeger AC (2009). Syndecan-1 regulates alphaVbeta3 and alphavbeta5 integrin activation during angiogenesis and is blocked by synstatin, a novel peptide inhibitor. J Exp Med 206, 691–705.

Carey DJ (1996). N-syndecan: structure and function of a transmembrane heparan sulfate proteoglycan. Perspect Dev Neurobiol 3, 331–346.

Chabot C, Spring K, Gratton JP, Elchebly M, Royal I (2009). New role for the protein tyrosine phosphatase DEP-1 in Akt activation and endothelial cell survival. Mol Cell Biol 29, 241–53.

Chaussade C *et al*. (2007). Evidence for functional redundancy of class IA PI3K isoforms in insulin signalling. Biochem J 404, 449–458.

Chen E, Hermanson S, Ekker SC (2002). Syndecan-2 is essential for angiogenic sprouting during zebrafish development. Blood 103, 1710–1719.

Choi S, Lee E, Kwon S, Park H, Yi JY, Kim S, Han IO, Yun Y, Oh ES (2005). Transmembrane domain-induced oligomerization is crucial for the functions of syndecan-2 and syndecan-4. J Biol Chem 280, 42573–42579..

Contreras HR, Fabre M, Granés F, Casaroli-Marano R, Rocamora N, Herreros AG, Reina M, Vilaró S (2001). Syndecan-2 expression in colorectal cancer-derived HT-29 M6 epithelial cells induces a migratory phenotype. Biochem Biophys Res Commun 286, 742–751.

Couchman JR (2003). Syndecans: proteoglycan regulators of cell-surface microdomains? Nat Rev Mol Cell Biol 4, 926–937.

Couchman JR (2010). Transmembrane signalling proteoglycans. Annu Rev Cell Dev Biol 26, 89–114.

Cuevas BD, Lu Y, Mao M, Zhang J, LaPushin R, Siminovitch K, Mills GB (2001). Tyrosine phosphorylation of p85 relieves its inhibitory activity on phosphatidylinositol 3-kinase. J Biol Chem 276, 27455–27461.

Destaing O, Sanjay A, Itzstein C, Horne WC, Toomre D, De Camilli CP, Baron R (2008). The tyrosine kinase activity of c-Src regulates actin dynamics and organization of podosomes in osteoclasts. Mol Biol Cell 19, 394–404.

Domin J, Harper L, Aubyn D, Wheeler M, Florey O, Haskard D, Yuan M, Zicha D (2005). The class II phosphoinositide 3-kinase PI3K-C2β regulates cell migration by a PtdIns(3)P dependent mechanism. J Cell Physiol 205, 452–462.

Domin J, Pages F, Volinia S, Rittenhouse SE, Zvelebil MJ, Stein RC, Waterfield MD (1997). Cloning of a human phosphoinositide 3-kinase with a C2 domain that displays reduced sensitivity to the inhibitor wortmannin. Biochem J 326, 139–147.

Essner JJ, Chen E, Ekker SC (2006). Syndecan-2. Int J Biochem Cell Biol 38, 152–156.

Ethell IM, Irie F, Kalo MS, Couchman JR, Pasquale EB, Yamaguchi Y (2001). EphB/syndecan-2 signaling in dendritic spine morphogenesis. Neuron 31, 1001–1013.

Ethell IM, Yamaguchi Y (1999). Cell surface heparan sulfate proteoglycan syndecan-2 induces the maturation of dendritic spines in rat hippocampal neurons. J Cell Biol 144, 575–586.

Fears CY, Gladson CL, Woods A (2006). Syndecan-2 is expressed in the microvasculature of gliomas and regulates angiogenic processes in microvascular endothelial cells. J Biol Chem 281, 14533–14536.

Folkes AJ *et al*. (2008). The identification of 2-(1H-indazol-4-yl)-6-(4-methanesulfonyl-piperazin-1-ylmethyl)-4-morpholin-4-yl-thieno[3,2-d] pyrimidine (GDC-0941) as a potent, selective, orally bioavailable inhibitor of class I PI3 kinase for the treatment of cancer. J Med Chem 51, 5522–5532.

Fox AN, Zinn K (2005). The heparan sulfate proteoglycan syndecan is an in vivo ligand for the *Drosophila* LAR receptor tyrosine phosphatase. Curr Biol 15, 1701–1711.

Galante LL, Schwarzbauer JE (2007). Requirements for sulfate transport and the diastrophic dysplasia sulfate transporter in fibronectin matrix assembly. J Cell Biol 179, 999–1009.

Gao Y, Li M, Chen W, Simons M (2000). Synectin, syndecan-4 cytoplasmic domain binding PDZ protein, inhibits cell migration. J Cell Physiol 184, 373–379.

Granés F, Urena JM, Rocamora N, Vilaró S (2000). Ezrin links syndecan-2 to the cytoskeleton. J Cell Sci 113, 1267–1276.

Grootjans JJ, Zimmerman P, Reekmans G, Smets A, Degeest G, Durr J, David G (1997). Syntenin, a PDZ protein that binds syndecan cytoplasmic domains. Proc Natl Acad Sci USA 94, 13683–13688.

Holsinger LJ, Ward K, Duffield B, Zachwieja J, Jallal B (2002). The transmembrane receptor protein tyrosine phosphatase DEP1 interacts with p120(ctn). Oncogene 21, 7067–7076.

Hsueh YP, Yang FC, Kharazia V, Naisbitt S, Cohen AR, Weinberg RJ, Sheng M (1998). Direct interaction of CASK/LIN-2 and syndecan heparan sulphate proteoglycan and their overlapping distribution in neuronal synapses. J Cell Biol 142, 139–151.

Imoto M, Kakeya H, Sawa T, Hayashi C, Hamada M, Takeuchi T, Umezawa K (1993). Dephostatin, a novel protein tyrosine phosphatase inhibitor produced by *Streptomyces*. I. Taxonomy, isolation, and characterization. J Antibiot (Tokyo) 46, 1342–1346.

Iuliano R, Le Pera I, Cristofaro C, Baudi F, Arturi F, Pallante P, Martelli ML, Trapasso F, Chiariotti L, Fusco A (2004). The tyrosine phosphatase PTPRJ/DEP-1 genotype affects thyroid carcinogenesis. Oncogene 23, 8432–8438.

Johnson KG *et al*. (2006). The HSPGs Syndecan and Dallylike bind the receptor phosphatase LAR and exert distinct effects on synaptic development. Neuron 49, 517–531.

Katso RM *et al*. (2006). Phospho-inositide 3-kinase C2β regulates cytoskeletal organization and cell migration via rac-dependent mechanisms. Mol Biol Cell 17, 3729–3744.
Keane MM, Lowrey GA, Ettenberg SA, Dayton MA, Lipkowitz S (1996). The protein tyrosine phosphatase DEP-1 is induced during differentiation and inhibits growth of breast cancer cells. Cancer Res 56, 4236–4243.
Kim CW, Goldberger OA, Gallo RL, Bernfield M (1994). Members of the syndecan family of heparan sulfate proteoglycans are expressed in distinct cell-, tissue-, and development-specific patterns. Mol Biol Cell 5, 797–805.
Klass CM, Couchman JR, Woods A (2000). Control of extracellular matrix assembly by syndecan-2 proteoglycan. J Cell Sci 113, 493–506.
Kovalenko M, Denner K, Sandström J, Persson C, Gross S, Jandt E, Vilella R, Böhmer F, Ostman A (2000). Site-selective dephosphorylation of the platelet-derived growth factor beta-receptor by the receptor-like protein-tyrosine phosphatase DEP-1. J Biol Chem 275, 16219–16226.
Kramer KL, Yost HJ (2002). Ectodermal syndecan-2 mediates left-right axis formation in migrating mesoderm as a cell-nonautonomous Vg1 cofactor. Dev Cell 2, 115–124.
Langford JK, Yang Y, Kieber-Emmons T, Sanderson RD (2005). Identification of an invasion regulatory domain within the core protein of syndecan-1. J Biol Chem 280, 3467–3473.
Marynen P, Zhang J, Cassiman JJ, Van den Berghe H, David G (1989). Partial primary structure of the 48- and 90-kilodalton core proteins of cell surface-associated heparan sulfate proteoglycans of lung fibroblastsPrediction of an integral membrane domain and evidence for multiple distinct core proteins at the cell surface of human lung fibroblasts. J Biol Chem 264, 7017–7024.
McFall AJ, Rapraeger AC (1997). Identification of an adhesion site within the syndecan-4 extracellular protein domain. J Biol Chem 272, 12901–12904.
McFall AJ, Rapraeger AC (1998). Characterization of the high affinity cell-binding domain in the cell surface proteoglycan syndecan-4. J Biol Chem 273, 28270–28276.
McQuade KJ, Beauvais DM, Burbach BJ, Rapraeger AC (2006). Syndecan-1 regulates alphaVbeta5 integrin activity in B82L fibroblasts. J Cell Sci 119, 2445–2456.
Morgan MR, Humphries MJ, Bass MD (2007). Synergistic control of cell adhesion by integrins and syndecans. Nat Rev Mol Cell Biol 8, 957–969.
Nightingale TD, Frayne ME, Clasper S, Banerji S, Jackson DG (2009). A mechanism of sialylation functionally silences the hyaluronan receptor LYVE-1 in lymphatic endothelium. J Biol Chem 284, 3935–3945.
Noguer O, Villena J, Lorita J, Vilaró S, Reina M (2009). Syndecan-2 downregulation impairs angiogenesis in human microvascular endothelial cells. Exp Cell Res 315, 795–808.
Okina E, Manon-Jensen T, Whiteford JR, Couchman JR (2009). Syndecan proteoglycan contributions to cytoskeletal organization and contractility. Scand J Med Sci Sports 19, 479–489.
Ostman A, Yang Q, Tonks NK (1994). Expression of DEP-1, a receptor-like protein-tyrosine-phosphatase, is enhanced with increasing cell density. Proc Natl Acad Sci USA 91, 9680–9684.
Ott VL, Rapraeger AC (1998). Tyrosine phosphorylation of syndecan-1 and -4 cytoplasmic domains in adherent B82 fibroblasts. J Biol Chem 273, 35291–35298.
Palka HL, Park M, Tonks NK (2002). Hepatocyte growth factor receptor tyrosine kinase met is a substrate of the receptor protein-tyrosine phosphatase DEP-1. J Biol Chem 278, 5728–5735.
Park H., Kim Y, Lim Y, Han I, Oh ES (2002). Syndecan-2 mediates adhesion and proliferation of colon carcinoma cells. J Biol Chem 277, 29730–29736.
Pera IL, Iuliano R, Florio T, Susini C, Trapasso F, Santoro M, Chiariotti L, Schettini G, Viglietto G, Fusco A (2005). The rat tyrosine phosphatase eta increases cell adhesion by activating c-Src through dephosphorylation of its inhibitory phosphotyrosine residue. Oncogene 24, 3187–3195..
Rodriguez F, Vacaru A, Overvoorde J, den Hertog J (2008). The receptor protein-tyrosine phosphatase, Dep1, acts in arterial/venous cell fate decisions in zebrafish development. Dev Biol 324, 122–130.
Ruivenkamp CA *et al*. (2002). Ptprj is a candidate for the mouse colon-cancer susceptibility locus Scc1 and is frequently deleted in human cancers. Nat Genet 31, 295–300.
Sallee JL, Burridge K (2009). Density-enhanced phosphatase 1 regulates phosphorylation of tight junction proteins and enhances barrier function of epithelial cells. J Biol Chem 284, 14997–15006.
Sanjay A *et al*. (2001). Cbl associates with Pyk2 and Src to regulate Src kinase activity, alpha(v)beta(3) integrin-mediated signaling, cell adhesion, and osteoclast motility. J Cell Biol 152, 181–195.
Saoncella S, Echtermeyer F, Denhez F, Nowlen JK, Mosher DF, Robinson SD, Hynes RO, Goetinck PF (1999). Syndecan-4 signals cooperatively with integrins in a Rho-dependent manner in the assembly of focal adhesions and actin stress fibres. Proc Natl Acad Sci USA 96, 2805–2810.
Senis YA *et al*. (2009). The tyrosine phosphatase CD148 is an essential positive regulator of platelet activation and thrombosis. Blood 113, 4942–4954.
Streuli CH, Akhtar N (2009). Signal co-operation between integrins and other receptor systems. Biochem J 418, 491–506.
Takahashi T, Takahashi K, St John PL, Fleming PA, Tomemori T, Watanabe T, Abrahamson DR, Drake CJ, Shirasawa T, Daniel TO (2003). A mutant receptor tyrosine phosphatase, CD148, causes defects in vascular development. Mol Cell Biol 23, 1817–1831.
Trapasso F *et al*. (2006). Genetic ablation of Ptprj, a mouse cancer susceptibility gene, results in normal growth and development and does not predispose to spontaneous tumorigenesis. DNA Cell Biol 25, 376–382.
Tsuboi N, Utsunomiya T, Roberts RL, Ito H, Takahashi K, Noda M, Takahashi T (2008). The tyrosine phosphatase CD148 interacts with the p85 regulatory subunit of phosphoinositide 3-kinase. Biochem J 413, 193–200.
Vanhaesebroeck B, Guillermet-Guibert J, Graupera M, Bilanges B (2010). The emerging mechanisms of isoform-specific PI3K signalling. Nat Rev Mol Cell Biol 11, 329–341.
Vepa S, Scribner WM, Natarajan V (1997). Activation of protein phosphorylation by oxidants in vascular endothelial cells: identification of tyrosine phosphorylation of caveolin. Free Radic Biol Med 22, 25–35.
Whiteford JR, Behrends V, Kirby H, Kusche-Gullberg M, Muramatsu T, Couchman JR (2007). Syndecans promote integrin-mediated adhesion of mesenchymal cells in two distinct pathways. Exp Cell Res 313, 3902–3913.
Whiteford JR, Couchman JR (2006). A conserved NXIP motif is required for cell adhesion properties of the syndecan-4 ectodomain. J Biol Chem 281, 32156–32163.
Whiteford JR, Ko S, Lee W, Couchman JR (2008). Structural and cell adhesion properties of zebrafish syndecan-4 are shared with higher vertebrates. J Biol Chem 283, 29322–29330.
Woods A, Longley RL, Tumova S, Couchman JR (2000). Syndecan-4 binding to the high affinity heparin-binding domain of fibronectin drives focal adhesion formation in fibroblasts. Arch Biochem Biophys 374, 66–72.